Lawrence Berkeley National Laboratory
Recent Work

Title

ANODIC DISSOLUTION OF IRON IN ACIDIC SULFATE ELECTROLYTES. PART II. MATHEMATICAL MODEL OF CURRENT OSCILLATIONS OBSERVED UNDER POTENTIOSTATIC CONDITIONS

Permalink

https://escholarship.org/uc/item/3jv7z6z4

Authors

Russell, P.
Newman, J.

Publication Date

1985-06-01

eScholarship.org Powered by the California Digital Library
University of California

LBL-19773
Preprint

Lawrence Berkeley Laboratory
UNIVERSITY OF CALIFORNIA

RECEIVED
LAWRENCE
BERKELEY LABORATORY
JUL 1 4 1986
LIBRARY AND
DOCUMENTS SECTION

Materials & Molecular Research Division

Submitted to the Journal of the
Electrochemical Society

ANODIC DISSOLUTION OF IRON IN ACIDIC SULFATE ELECTROLYTES. Part II. MATHEMATICAL MODEL OF CURRENT OSCILLATIONS OBSERVED UNDER POTENTIOSTATIC CONDITIONS

P. Russell and J. Newman

June 1985

TWO-WEEK LOAN COPY
This is a Library Circulating Copy
which may be borrowed for two weeks.

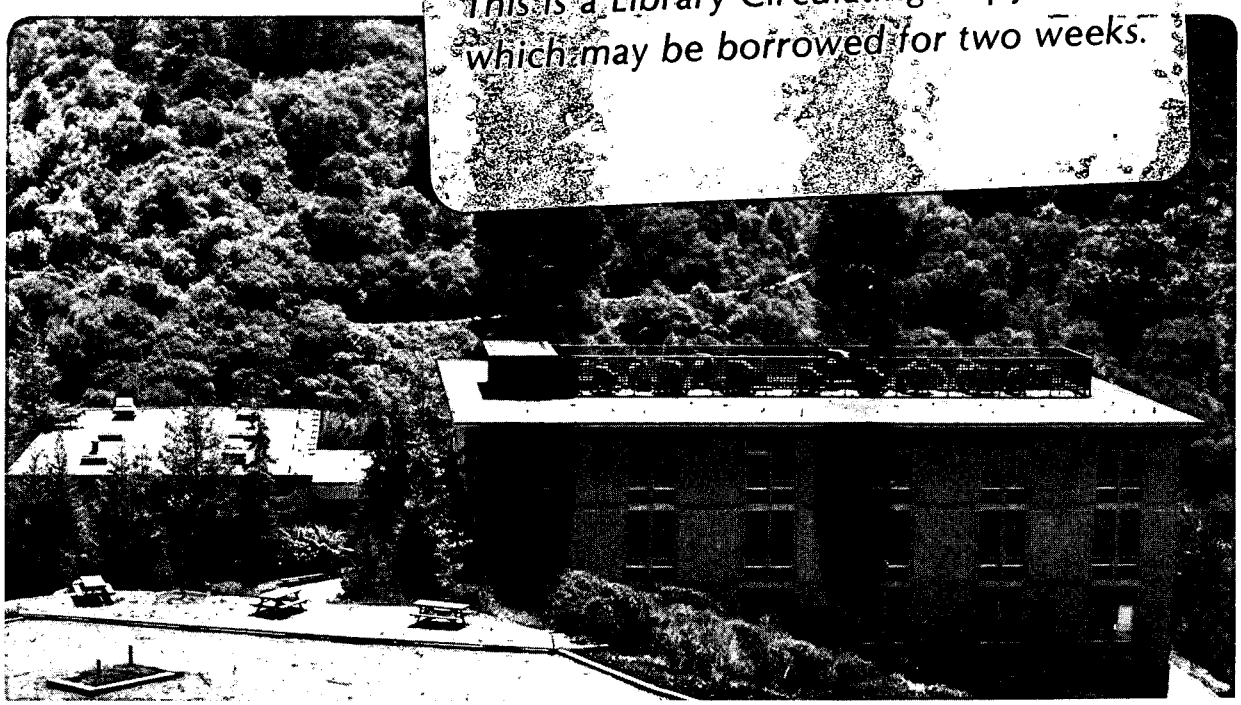

Prepared for the U.S. Department of Energy under Contract DE-AC03-76SF00098

LBL-19773
c.2

DISCLAIMER

This document was prepared as an account of work sponsored by the United States Government. While this document is believed to contain correct information, neither the United States Government nor any agency thereof, nor the Regents of the University of California, nor any of their employees, makes any warranty, express or implied, or assumes any legal responsibility for the accuracy, completeness, or usefulness of any information, apparatus, product, or process disclosed, or represents that its use would not infringe privately owned rights. Reference herein to any specific commercial product, process, or service by its trade name, trademark, manufacturer, or otherwise, does not necessarily constitute or imply its endorsement, recommendation, or favoring by the United States Government or any agency thereof, or the Regents of the University of California. The views and opinions of authors expressed herein do not necessarily state or reflect those of the United States Government or any agency thereof or the Regents of the University of California.

LBL-19773

Anodic Dissolution of Iron in Acidic Sulfate Electrolytes

Part II: Mathematical Model of Current Oscillations Observed under Potentiostatic Conditions

Philip Russell and John Newman

Materials and Molecular Research Division
Lawrence Berkeley Laboratory
and
Department of Chemical Engineering
Univeristy of California
Berkeley, California 94720

June 1985

LBL-19773

Anodic Dissolution of Iron in Acidic Sulfate Electrolytes

Part II: Mathematical Model of Current Oscillations Observed under Potentiostatic Conditions

Philip Russell[1,*] and John Newman[*]

Materials and Molecular Research Division,
Lawrence Berkeley Laboratory, and
Department of Chemical Engineering,
University of California, Berkeley, California 94720

June, 1985

Abstract

A mathematical model describing sustained current oscillations observed in the iron-sulfuric acid system, under potentiostatic conditions, is presented. It is assumed that the sustained oscillations are due to a continuous cycling of the electrode between the active and the passive states. The electrode surface is covered by a porous ferrous sulfate film. Transient changes in the potential and concentration profiles in the pores of the salt film and in the diffusion layer are responsible for the continuous cycling. A one-dimensional model that describes these processes is presented. Results from this model are compared to the experimental current-time curves. The shape of the calculated current-time curve qualitatively agrees with experiment. The calculated ferrous sulfate film thickness is substantially thinner than expected from a steady-state analysis and from the previously reported work of others.

Three modifications that may bring the calculated results more in line with experimental results are qualitatively outlined. These modifications suggest that one may wish to: (i) include kinetics of salt-film dissolution in the model, it is anticipated that this will increase the calculated salt-film thickness; (ii) remove the requirement of passivation, and assume that the current oscillations are caused by continuous cycling in the fraction of the

electrode surface area that is covered by ferrous sulfate; (iii) remove the requirement of passivation, and assume that the current oscillations are caused by continuous cycling in the porosity of the salt film.

---

[1]Present address: Weyerhaeuser Technology Center, Tacoma, Washington 98477.

*Electrochemical Society Active Member

Key words: mass transport, corrosion, kinetics.

This paper begins with a brief review of the literature concerning mathematical models describing electrochemical oscillations. It is assumed that oscillations are due to a continuous cycling between the active and the passive states. The passivation potential is a function of the pH at the electrode-salt film interface. This dependence is expressed in a quantitative manner. Next, the steady-state limiting current is studied. Relationships that must exist between the salt-film thickness, the salt-film porosity, the fraction of the electrode surface covered by precipitated $FeSO_4$, and the potential are determined and presented in the form of a nomograph. We then discuss the probable radial variations in the potential profile, the concentration profiles, and the salt-film thickness. This is done to obtain an appreciation for the severity of the approximations that are made when radial variations are ignored, which is the case for the one dimensional model developed here. A qualitative description of the proposed physical processes that lead to sustained current oscillations is then given. The system of fundamental equations that were developed in Part I of this series[1] are used to simulate these physical processes. The boundary conditions for these differential equations require some modification from the forms presented in the salt-film growth model,[1] and these changes are discussed. Finally, the resulting oscillation frequencies and current-time wave forms are presented and compared with experimental data.

The results of this model indicate that increasing surface coverage due to precipitated $FeSO_4$ on the electrode surface is responsible for a larger decrease in current than is possible from the formation of a passivated peripheral region alone. Therefore, two alternative oscillatory mechanisms are outlined and recommended for future study. One mechanism is based on periodic changes in the fraction of the electrode surface area that is covered with precipitated $FeSO_4$, and the other is based on periodic changes in the

salt-film porosity.

Summary of previous models

A comprehensive review article by Wojtowicz[2] summarizes many of the theories proposed to explain oscillatory phenomena.

Several methods are available for the solution of sets of equations describing nonlinear oscillations. Wojtowicz[2] presents a "phase-plane" analysis for systems that can be described by two autonomous equations,

$$\frac{dx}{dt} = P(x,y), \text{ and } \frac{dy}{dt} = Q(x,y). \quad (1)$$

The system is autonomous if P and Q are independent of t. The method of isoclines[3] may be used to determine graphically the trajectories in the phase-plane portrait of such a system when P and Q are nonlinear functions. If P and Q are linear functions, the shape of the trajectories is determined by the nature of the roots of the characteristic equation derived from Equation (1). Sustained oscillations result only when the roots of the characteristic equation are pure imaginary numbers. This type of behavior is known as a "center."

In nonlinear systems, the shape of trajectories far away from the steady state point are important in determining whether or not the system will exhibit sustained oscillations. Unlike linear systems, nonlinear systems can develop trajectories known as limit cycles.

A limit cycle is a closed trajectory such that no trajectory in the close neighborhood of it is also closed.[2,3] Every trajectory from the surrounding regions either winds itself into the limit cycle as $t \to \infty$ (a stable limit cycle), or unwinds from it (an unstable limit cycle). Unlike oscillations around a center, limit cycles represent sustained oscillations which are determined by the governing differential equations, and are independent of the initial conditions.

Relaxation oscillations

Relaxation, or discontinuous, oscillations characterize periodic behavior of systems that cannot be described by continuous and differentiable functions. Their phase-plane representation is characterized by very fast movements along some sections of the cycle. The fundamentals of relaxation oscillations are outlined by Wojtowicz.[2] Further detail can be obtained from texts concerning nonlinear oscillations, such as Minorsky.[4]

Other mathematical tools used to describe oscillatory behavior have been developed. Many techniques, such as perturbation, bifurcation,[5] and asymptotic methods, although available,[4] are not described here.

A summary of some specific models is now presented.

Model of Franck and FitzHugh[6]

The case of iron polarized at constant potential is considered. The following assumptions are made:

(1) An oxide film is formed on the electrode when $\hat{x} > 0$ and dissolves when $\hat{x} < 0$, where $\hat{x}$ is given by $\hat{x} = V - V_F$. Here, V_F is the Flade potential under the existing conditions, and V is the electrode potential which is held constant relative to a reference electrode. The rate of film formation is proportional to the free area of the electrode, $(1 - \Theta)$, and the rate of film dissolution is proportional to the coverage, Θ.

(2) At the uncovered part of the electrode, dissolution occurs when $\hat{x} < 0$.

(3) Partial currents of both reactions depend linearly on the potential.

(4) The Flade potential depends logarithmically on the H^+ concentration.

(5) In the electrolyte, H^+, Fe^{++}, and SO_4^{--} ions carry the current.

(6) The H^+ concentration profile in the diffusion layer is always linear.

(7) The rate of production of H^+, which accompanies formation of the oxide, is neglected in comparison with transport fluxes.

A phase plane analysis results in a stable limit cycle when the potential difference, $\hat{x}$, is plotted as a function of the surface coverage. The result is significant in that oscillatory behavior is obtained. However, there is no discussion of the effect that changing the input parameters has on the frequency and amplitude of the oscillations. Also, formation of a ferrous sulfate salt film as a precursor to passivation is absent from this model. Several authors[7-9] have shown the importance of salt-film formation as a precusor to oxide passivation for iron in acidic electrolytes.

This is an example of a "chemical" model. By "chemical," it is meant that the kinetics of reactions together with mass transport processes must be solely responsible for the oscillations. So called "electrical" models have also been developed. In this context, an electrode is explicitly treated as an element of the circuit and is described either by its current-voltage characteristics or by an equivalent circuit. An illustration of an "electrical" model follows.

Model of Degn[10]

A model based on ohmic resistance, passivation, and concentration overpotential is proposed to account for periodic behavior. The following assumptions are made:

(1) The potential of the electrode is defined by the equilibrium electrosorption of species A on free sites, S; that is,

$$V - \Phi_o = U^\theta - U^\theta_{ref} - \frac{RT}{F} \ln ([A][S]/[AS]) . \qquad (2)$$

The fraction of unoccupied sites is given by

$$1 - \Theta = 1/(1 + A \exp [F((V - \Phi_o) - (U^\theta - U^\theta_{ref}))/RT]) \qquad (3)$$

or, approximately, by

$$1 - \Theta = k_4/(k_5(V - \Phi_o)^2 + 1) . \tag{4}$$

(2) Diffusion effects are accounted for by assuming that the current is proportional to $1 - \Theta$ and to $(V - \eta_c)$, where η_c is the concentration overpotential, that is,

$$I = k_1(1 - \Theta)(V - \eta_c) . \tag{5}$$

Polarization increases linearly with current, while the simultaneously occurring tendency for diffusion to decrease the concentration gradient is a first order process. This gives

$$\frac{d\eta_c}{dt} = k_2 I - k_3\eta_c . \tag{6}$$

(3) The cell voltage, V- Φ_{RE}, and an ohmic resistance, R, are both taken to be constants giving

$$V - \Phi_{RE} = V - \Phi_o + IR . \tag{7}$$

Combining Equations (4), (5), and (7) gives

$$\eta_c = \frac{k_5}{k_1 k_4}\left\{-R^2I^3 + 2(V - \Phi_{RE})RI^2 - I(V - \Phi_{RE})^2 - \frac{I}{k_5}\right\} - IR + V - \Phi_{RE} . \tag{8}$$

If it is assumed that $k_1 = k_4 = k_5 = 1$, then, for certain values of R and $V - \Phi_{RE}$, the current, I, is a three-valued function of η_c. The three-valued nature of the current leads to relaxation oscillations. An analog computer simulation resulted in an oscillatory current-time plot.

Again, with this model, a salt film is not included; and, as with all electrical models, the true behavior of the system may be lost in the arbitrary process of selecting the current-voltage characteristics of the electrode.

Model of Cooper *et al.*[11]

Voltage oscillations at a copper electrode undergoing galvanostatic dissolution are considered. Their study involved copper, and this model concerns iron; therefore, the mechanistic details of their model are not considered here. The outstanding feature of their model is a detailed explanation of why oscillations are expected, and why the simple case of the system moving to a steady state determined by the rate limiting step does not occur. It is important for any proposed model to be able to explain why oscillations, and not a steady state, are expected.

Model of Podesta *et al.*[12]

Podesta *et al.* observed two different types of oscillatory behavior. The dividing criterion for these two types of oscillations is a H_2SO_4 concentration of 1.0 M. For H_2SO_4 concentrations greater than 1.0 M, a dissolution-precipitation mechanism is controlling. For this case, oscillations cease if the solution is stirred. Since the oscillations observed in the present work occurred under vigorous stirring, their "low acid concentration" model is most pertinent for comparison with these experimental results.

Two different rates of current decay are observed in the active region. Initially, the current decay is gradual; the charge passed is mainly assigned to metal electrodissolution. Later in the cycle, the current decay is much more rapid. A portion of the charge passed is used to form anodic products involved in metal passivation; the balance of the charge passed results in further metal dissolution.

It is imagined that a potential step is made which puts the electrode into a region where oscillations occur. Initially, there is anodic dissolution of the metal. The kinetics of iron dissolution govern this process, and they have been studied extensively.[13-17] The high rate of iron dissolution implies a

simultaneous accumulation of Fe^{++} ions near the electrode surface and the migration of H^+ ions out of this region. The resulting exchange of H^+ ions for Fe^{++} ions favors hydrolysis of Fe^{++} and precipitation of $Fe(OH)_2$ as the initial dissolution inhibiting species. This process results in a steady decrease in current. The degree of hydrolysis depends on the proton migration current and the ratio of cation concentration to hydrogen ion concentration.

The second decrease in current in the active region is due to film thickening and structural changes. Certain oxy-hydroxo-species are presumed to form within the layer. At this point, the anodic current has decreased drastically. This allows the compositions near the interface to approach those of the bulk solution. The increased acid concentration promotes the chemical dissolution of the oxy-hydroxo-hydrated passivating films. It has been observed that the passive region is more strongly influenced by the rate of stirring than the active region.[18] This indicates a significant mass transfer contribution in the film dissolution phase of the process. At this point the cycle repeats itself.

Conditions for passivation

The oscillations are caused by the electrode making continuous transitions between the active and the passive states. Several authors have demonstrated that salt-film formation is a necessary precursor to oxide passivation for iron in sulfuric acid solutions.[7-9] For these reasons, a porous ferrous sulfate salt film will be included as an integral part of the model to be proposed here.

We must know what conditions allow the electrode to be in the active state, and what conditions force the electrode to be in the passive state.

Pourbaix[19] has presented data showing the dependence of the passivation potential on pH; this is reproduced in Figure 1. The

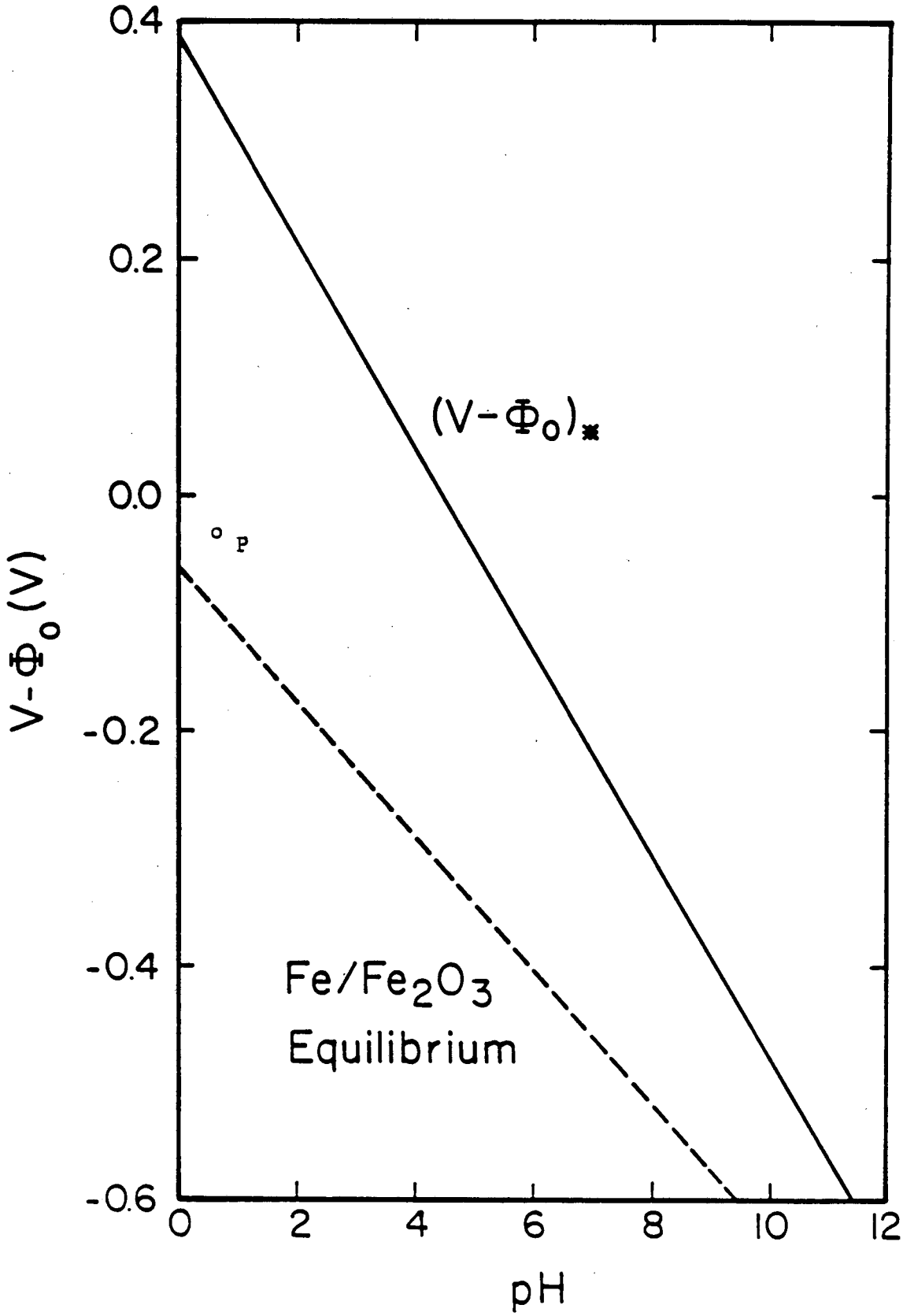

Figure 1. Experimentally determined potential-pH passivation conditions and the theoretical equilibrium between Fe and Fe_2O_3 (dashed line) taken from Pourbaix.[19]

thermodynamic equilibrium between Fe and Fe_2O_3 is also shown on Figure 1 as the dashed line. The system requires higher potentials at a given pH, or higher pH values at a given potential, to passivate than one might expect from the equilibrium conditions.

For the remainder of this paper, all potentials will be measured relative to a normal hydrogen electrode (NHE).

Russell and Newman[20] have shown that the passive-active transition occurs at $V - \Phi_{NHE} = +0.423$ V for iron in a 1 M H_2SO_4 electrolyte. The surface pH was estimated to be 0.3 when the active-passive transition occurred. This result confirms that the experimental line on Figure 1 correctly represents the division between the active and the passive states.

The results from Part I of this series indicated the potential and pH conditions near the electrode surface at the instant the salt film began to form. At t_{o+}, $(V - \Phi_o)$ = -0.028 V, and the surface pH is 1.08 for a surface porosity of 0.01; these conditions are represented by point P on Figure 1. The location of point P depends on the initial value of the surface porosity. For values of ϵ_s less than 0.60, the conditions for initial film formation will lie above the Fe/Fe_2O_3 equilibrium line. This result is obtained with the assumption that the initial surface pH value is independent of the initial surface porosity value, so that only the value of $(V - \Phi_o)$ is affected. The salt film has just begun to form, and the experimental results indicate that the electrode is in the active state. Since point P is above the thermodynamic equilibrium line for any ϵ_s less than 0.60, it is unlikely that this line represents the division between the active and the passive states. This fact, again, indicates that the upper line on Figure 1 is correct. The upper line on Figure 1 is represented by

$$(V - \Phi_o)_* = 0.385 - 0.0862\ \mathrm{pH} \quad . \tag{9}$$

Steady-state conditions

It is helpful to consider the steady-state conditions at various cell potentials on the limiting-current plateau before discussing the processes leading to oscillations. The electrode is assumed to be covered by a salt film at all potentials on the limiting-current plateau. Specifically, we want to consider the relationships that must exist between the salt-film thickness, the salt-film porosity, and the fraction of the electrode surface that is covered by precipitated salt crystals in the absence of any complications due to the oscillations.

Let us begin by considering the curve for Ω = 167.6 rad/s on Figure 2. The limiting current has a value of 1.3 A/cm^2. The limiting-current plateau is observed to exist between 0.465 V and 0.765 V, relative to a NHE.

We assume that a certain fraction of the electrode surface is free, that is, not covered by the precipitated salt crystals. This free fraction is called the surface porosity, ϵ_s, and has been included in the salt-film formation problem outlined in Part I of this series. The superficial current density is constant at 1.3 A/cm^2 on the plateau. Given a value of ϵ_s, one may calculate a value of the Butler-Volmer current density:

$$i_{bv} = i/\epsilon_s \,. \tag{10}$$

Equation (I-28)* may be inverted to solve for the value of $(V - \Phi_o)$ that is consistent with this current density. Neglecting the cathodic term in Equation (I-28) permits this inverted equation to be expressed as

$$(V - \Phi_o) = \frac{RT}{\alpha_a F} \ln \frac{i_{bv}}{nFk_a} = \frac{RT}{\alpha_a F} \ln \frac{i/\epsilon_s}{nFk_a} \,. \tag{11}$$

This relationship is plotted in part A of Figure 3. Decreasing values of ϵ_s require increases in $(V - \Phi_o)$ so that the product $\epsilon_s i_{bv}$ is maintained at the

*Any equation number preceded by an "I-" refers to the equation with the given number in Part I of this series.

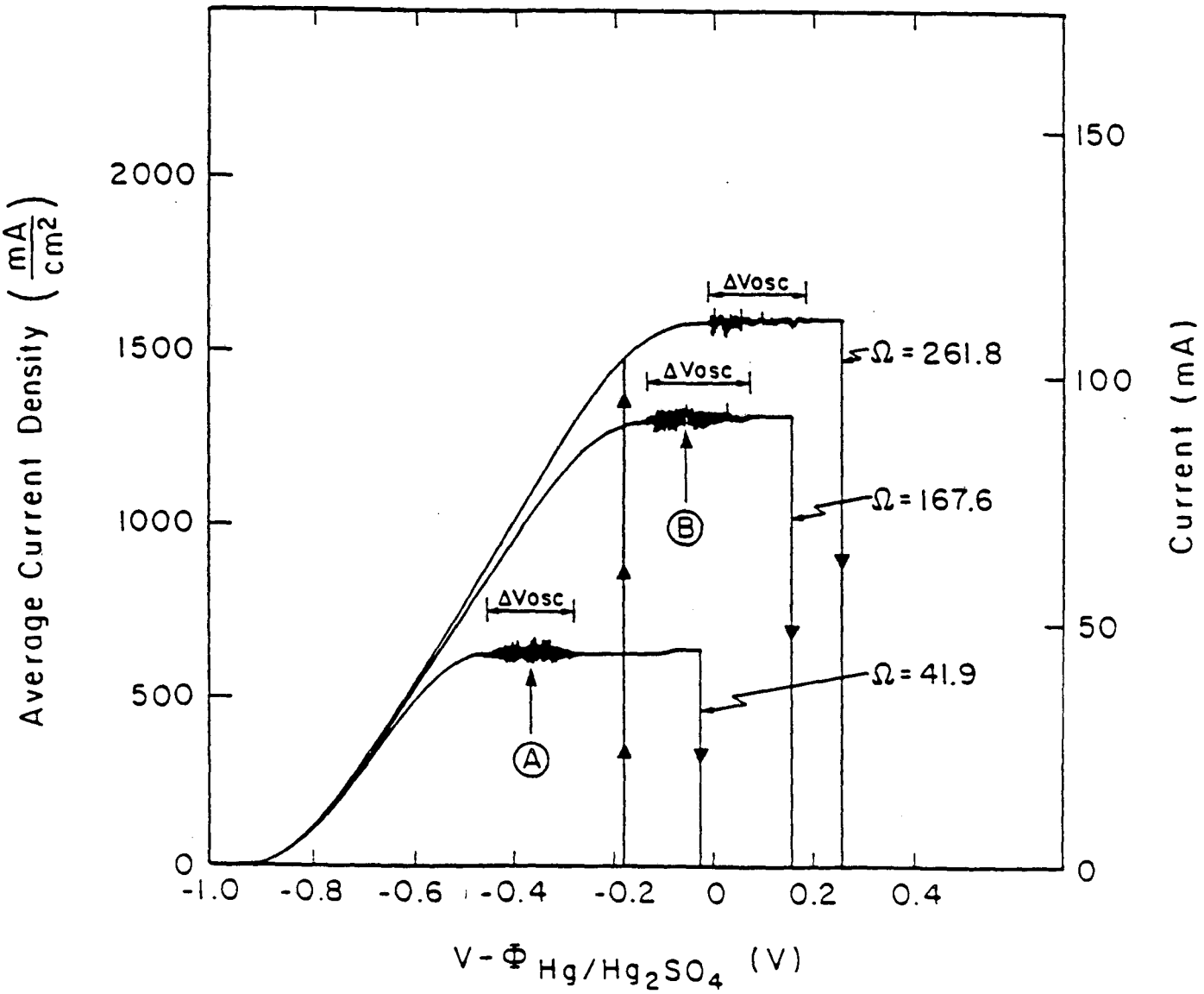

Figure 2. Potentiodynamic sweep curves for a rotating disk electrode, with radius = 0.149 cm, in a 1 *M* H_2SO_4 electrolyte. Regions in which oscillations are observed are indicated. For clarity, the current overshoot phenomenon is not shown. The potential difference between a mercury-mercurous sulfate reference electrode and a normal hydrogen electrode is given by $\Phi_{Hg/Hg_2SO_4} - \Phi_{NHE} = 0.61515$ V.[21]

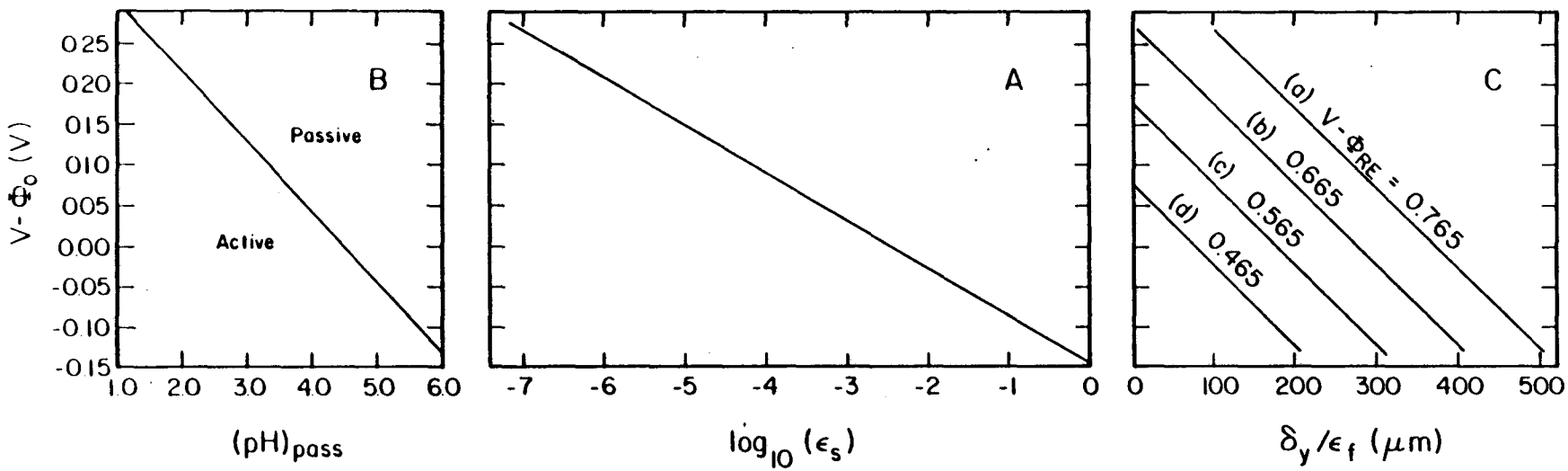

Figure 3. Steady-state limiting current analysis. Part A, value of $(V - \Phi_o)$ required to produce i_L at various values of ϵ_s. Part B, value of the surface pH which will result in passivation at a given value of $(V - \Phi_o)$ based on the experimentally determined passivation curve in Figure 1. Part C, values of δ_y/ϵ_f for various cell potentials at given values of $(V - \Phi_o)$.

limiting-current value.

When $V - \Phi_{RE}$ = 0.765 V, the system is on the verge of passivation (see Figure 2). This must be true because a slight increase in cell potential results in immediate passivation. Equation (9) provides the value of the surface pH which must exist at the electrode-salt film interface at this cell potential. This relationship is shown in part B of Figure 3. At a given value of $(V - \Phi_o)$, the electrode will be in the active state for surface pH values that are to the left of the diagonal line. The electrode will passivate if the surface pH is to the right of this line.

We now determine possible values of the salt-film thickness and the salt-film porosity. An approximate potential balance is:

$$V - \Phi_{RE} = (V - \Phi_o) + \Delta\Phi_{d,f} + \frac{i}{\kappa_f}\left(\frac{\delta_y}{\epsilon_f}\right) + \Delta\Phi_{d,s} + i\frac{\pi r_o}{4\kappa_{H_2SO_4}}. \qquad (12)$$

The second term on the right is the diffusion potential associated with concentration gradients contained within the pores of the salt film. For $V - \Phi_{RE}$ = 0.765 V, this term is estimated by the Henderson[22,23] equation to have a value of 0.008 V. The third term represents the ohmic potential drop in the pores of the salt film. This term is proportional to the salt-film thickness and the superficial current density and inversely proportional to the conductivity of the solution in the pores and the porosity of the salt film. κ_f is estimated to have a value of 0.132 Ω^{-1}–cm^{-1}. This value is based on a low hydrogen ion concentration, which is due to migration of H^+ out of the salt film. Reduced ionic mobilities, due to the concentrated solutions that are expected in the salt-film pores, are also taken into account in arriving at this value. The fourth term on the right side is the diffusion potential in solution. Again, the Henderson equation has been used to estimate a value of this term, with a result of 0.008 V. The fifth term is the ohmic potential drop between the salt film-solution interface and a hemispherical counterelectrode located

at infinity, where the conductivity is assumed to be constant and equal to the bulk value.

With these assumptions, one may calculate a value of δ_y/ϵ_f for values of $V-\Phi_{RE}$ and ϵ_s. Fixing $V-\Phi_{RE}$ at 0.765 V, but varying ϵ_s (and therefore varying $(V-\Phi_o)$) allows values of δ_y/ϵ_f to be calculated. These results are shown as line (a) on part C of Figure 3. Equation (12) was slightly modified for values of $V-\Phi_{RE}$ less than 0.765 V. At a given value of $(V-\Phi_o)$, the ratio δ_y/ϵ_f must decrease as the value of $V-\Phi_{RE}$ decreases. A decrease in δ_y/ϵ_f should result in a reduction of the diffusion potential in the pores of the salt film. As a rough approximation, we assume that the diffusion potential in the pores of the salt film is linearly proportional to δ_y/ϵ_f. With this assumption, Equation (12) becomes

$$V-\Phi_{RE} = (V-\Phi_o) + \frac{\delta_y/\epsilon_f}{(\delta_y/\epsilon_f)_\bullet}\Delta\Phi_{d,f} + \frac{i}{\kappa_f}\left(\frac{\delta_y}{\epsilon_f}\right) + \Delta\Phi_{d,s} + i\frac{\pi r_o}{4\kappa_{H_2SO_4}}, \qquad (12a)$$

where $(\delta_y/\epsilon_f)_\bullet$ is the value of δ_y/ϵ_f obtained with $V-\Phi_{RE} = 0.765$ and at the given value of $(V-\Phi_o)$. Results from Equation (12a) for values of $V-\Phi_{RE}$ = 0.665, 0.565, and 0.465 V are shown as lines (b), (c), and (d), respectively, on part C of Figure 3.

These plots permit one to estimate the value of δ_y/ϵ_f at a given cell potential for various values of ϵ_s. As an example, assume $\epsilon_s = 10^{-2}$. Moving up the graph in part A of Figure 3, we see that a value of $(V-\Phi_o)$ = -0.028 V is required to keep the superficial current density at the limiting value. At this value of $(V-\Phi_o)$, part B indicates that the electrode surface will be in the active state as long as the pH at the electrode-salt film interface remains less than 4.8.

Move to the right along the line where $(V - \Phi_o)$ = -0.028 V to part C of the drawing. We see that δ_y/ϵ_f would have values of 105, 204, 303, and 402 μm for $V - \Phi_{RE}$ equal to 0.465, 0.565, 0.665, and 0.765 V, respectively.

Figure 3 will be used to determine whether the calculated results from the model are physically realistic. We will employ it when oscillatory results are presented later in this paper.

Radial variations

The current oscillations observed in the potential range ΔV_{osc} (Figure 2) are caused by the electrode continuously making the transition between the active and the passive states. Figure 4 illustrates the current-time curve for 167.6 rad/s. The maximum current density on a given cycle is obtained when all or most of the electrode surface is in the active state. The minimum current density represents a partly active-partly passive state. The minimum current density is too large to be produced by an entirely passivated electrode. A certain portion of the electrode surface always undergoes active dissolution. We wish to determine if this perpetually active region is located near the center of the electrode, in which case the periphery undergoes transitions between the active and the passive states, or if the periphery is always active, in which case the central region undergoes transitions between the two states.

In this section, we relax our previous assumption of a one dimensional geometry, and consider the effect of radial variations. This discussion should make clear what is being neglected when we return to the one dimensional problem.

A schematic diagram of the electrode and the salt film is given in Figure 5, part (a). A similar drawing indicating possible potential distributions is shown in part (b) of this figure.

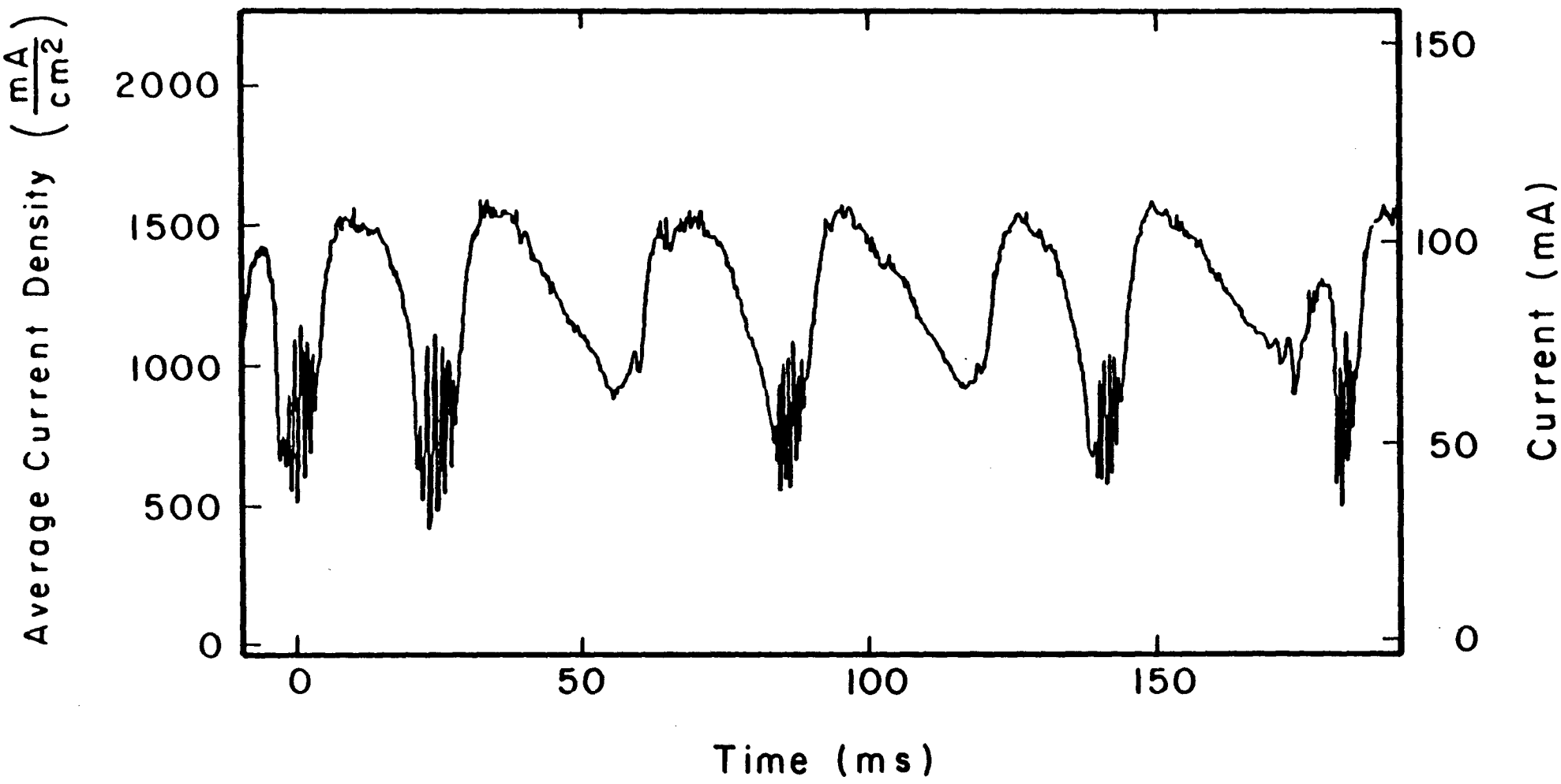

Figure 4. Sustained oscillations observed for a disk electrode with a radius of 0.149 cm in a 1 *M* H_2SO_4 electrolyte at $\Omega = 167.6$ rad/s. The electrode is polarized at a potential near the center of ΔV_{osc} on Figure 2.

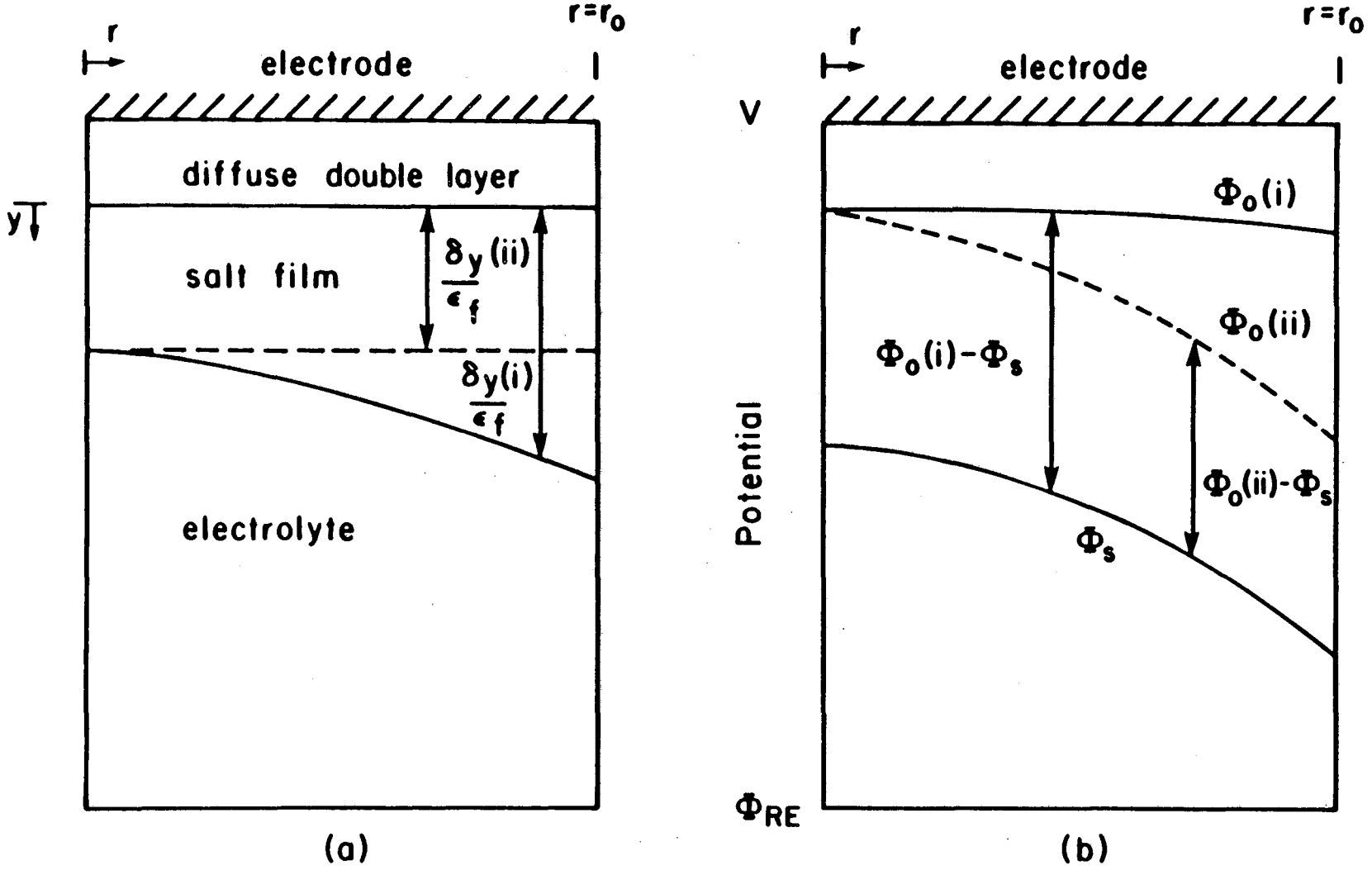

Figure 5 Radial variations for a salt film covered disk electrode. Part (a), variations in δ_y / ε_f. Part (b), variations in Φ_o and Φ_s.

The limiting current is assumed to result from a uniform current density distribution over the surface of the disk. Φ_s is the potential at the salt film-solution interface, measured with respect to a distant reference electrode of a given kind. For a uniform current density, Φ_s is larger at the center of the disk than near the edge.[24]

Consider two cases:

(*i*) the surface porosity is constant on the surface of the electrode.

(*ii*) the surface porosity decreases with increasing radial position.

In case (*i*), Φ_o must be nearly constant in order that the superficial current density remain constant. This requires that the potential drop through the porous salt film be larger near the periphery than near the center. This can be seen on Figure 5, part (b) by the distance between $\Phi_o(i)$ and Φ_s. The potential drop through the salt film is the sum of an ohmic component and diffusion potential component. Assume that both of these components increase with radial position. For the ohmic component to increase, δ_y/ϵ_f must be larger near the periphery than near the center. If ϵ_f is constant, then the salt film must be thicker near the periphery than it is near the center. This is shown in Figure 5, part (a) by the line labeled $\delta_y(i)/\epsilon_f$. For the diffusional component to increase, the pH change through the salt film must be larger near the periphery than near the center. The surface pH will be largest at the periphery and smallest at the center. Referring to Figure 1, it is found that the periphery will passivate preferentially to the center for case (*i*) because of the larger surface pH.

In case (*ii*), the surface porosity is decreasing as r increases. To maintain a constant superficial current density, the Butler-Volmer current density must increase with radial position. This requires Φ_o to decrease with radial position. This permits $(V - \Phi_o)$, the driving force in the Butler-Volmer equation, to increase. $\Phi_o(ii)$ is shown as the dashed curve on Figure 5, part

(b). The potential drop through the salt film, $\Phi_0(ii) - \Phi_s$, is now more nearly constant from center to edge. The value of δ_y/ϵ_f will also be more nearly constant from center to edge, as shown by the dashed line in Figure 5, part (a). Returning to Figure 5, part (b), we see that $V - \Phi_0(ii)$ is largest near the periphery; therefore, the electrode will preferentially passivate near the edge.

In both cases, the electrode will preferentially passivate near the edge, while the central portion of the disk remains active. The mathematical model describes a location on the electrode near the periphery that is subjected to the continuous transitions between the active and the passive states. We will describe how the current flowing from the central active portion of the electrode influences the value of Φ_0 on the passivated portion of the electrode later in this paper.

Qualitative description of the physical phenomena

It is assumed that a porous ferrous sulfate salt film covers the electrode. The process that leads to initial salt-film formation is referred to as phase 1 and has been described in Part I of this series.

The diagonal line on Figure 6 indicates the experimentally observed division between the active and the passive states.[19] The electrode is in the active state for potential and pH combinations that lie below this line. In the active state, the porous salt film covers the electrode. This is indicated by the schematic in the lower left corner of Figure 6. High rate dissolution occurs with released ferrous ions moving through the film pores by migration and diffusion and then moving into the electrolyte. Formation of a nonporous Fe_2O_3 film occurs for potential and pH combinations lying above the diagonal line on Figure 6; this is the passive state. The oxide layer is assumed to have a thickness of several monolayers or less. The oxide layer forms below the

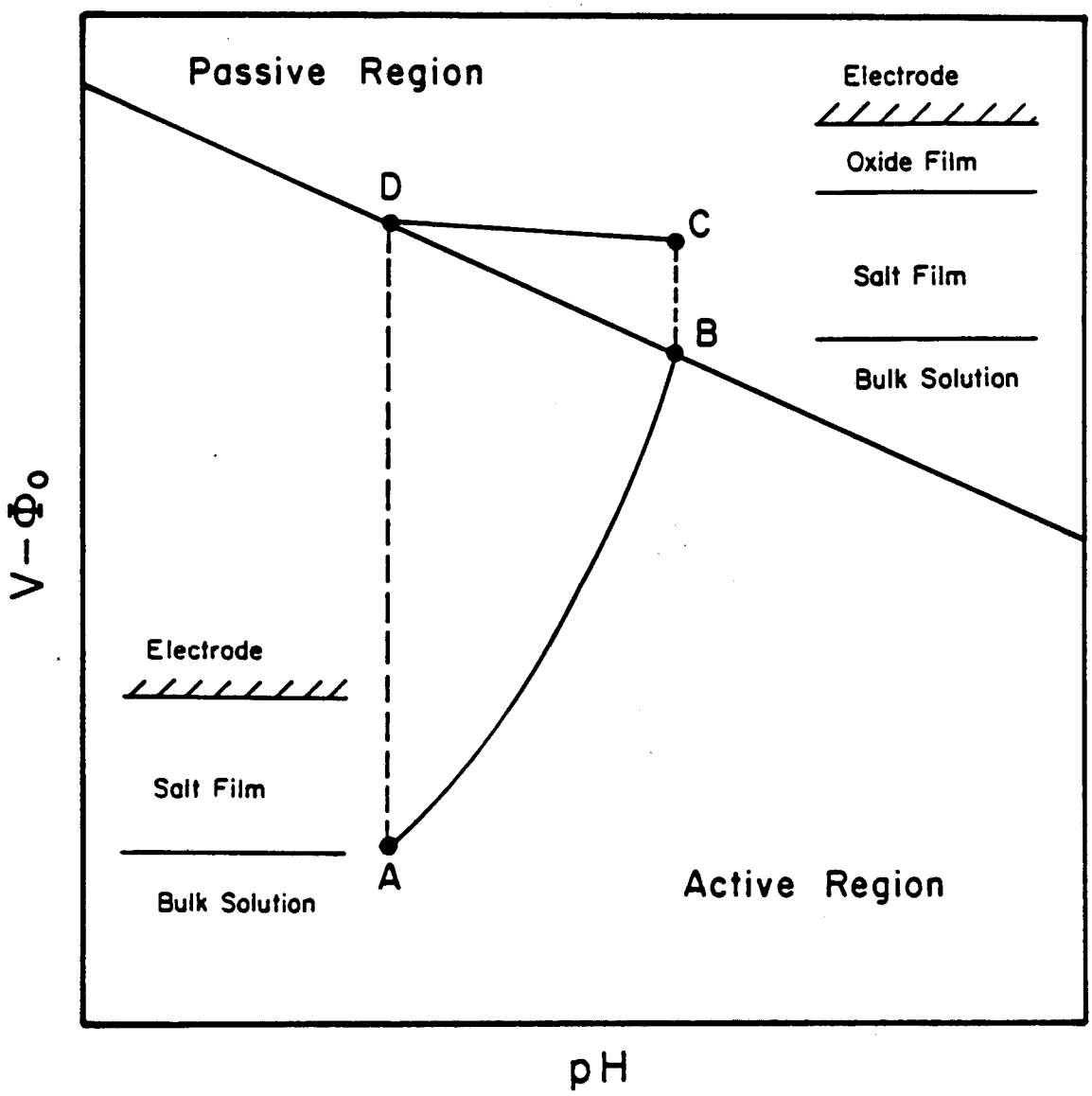

Figure 6. Potential-pH diagram illustrating the changing conditions at the electrode surface during a typical cycle.

salt-film layer, directly on the electrode surface, as shown by the schematic on the upper right in Figure 6. The current density has a near zero value in the passive state, relative to the active state.

Assume the electrode is in the active mode, point A on Figure 6. The high current density associated with active dissolution results in a large potential gradient in the pores of the salt film. The large potential gradient causes hydrogen ions to migrate transiently out of the pores of the salt film. This process is shown in Figure 7. The pH at the film-electrode interface increases. A transient increase in the ferrous ion concentration also occurs in the pores of the salt film. The rising ferrous concentration in the pores leads to increased rates of $FeSO_4$ precipitation, especially near the electrode-salt film interface where concentrations are largest. A decrease in the surface porosity results. Increased surface blockage will lower the superficial current density; however, the value of $(V - \Phi_o)$ will increase.* These processes are referred to as phase 2 and are characterized by line AB on Figure 6.

Sufficient increase in the surface pH and $(V - \Phi_o)$ results in passivation at point B. A covering oxide film forms on the electrode surface, underneath the porous salt film. There is a sharp decrease in current density when the electrode passivates. The ohmic potential drop between the working electrode and the reference electrode is decreased. This results in an instantaneous increase in $(V - \Phi_o)$ to point C on Figure 6.

The jump in $(V - \Phi_o)$ may be visualized in Figure 8. The potential difference between the disk and the reference electrode is a constant. The ohmic potential drop for the high current density active state is large; this results in a small value for $(V - \Phi_o)$. The ohmic drop for the low current

*This is the same phenomenon that occurred when the salt film initially formed on the electrode surface. See Figure 8 in Part I of this series and the associated discussion for clarification.

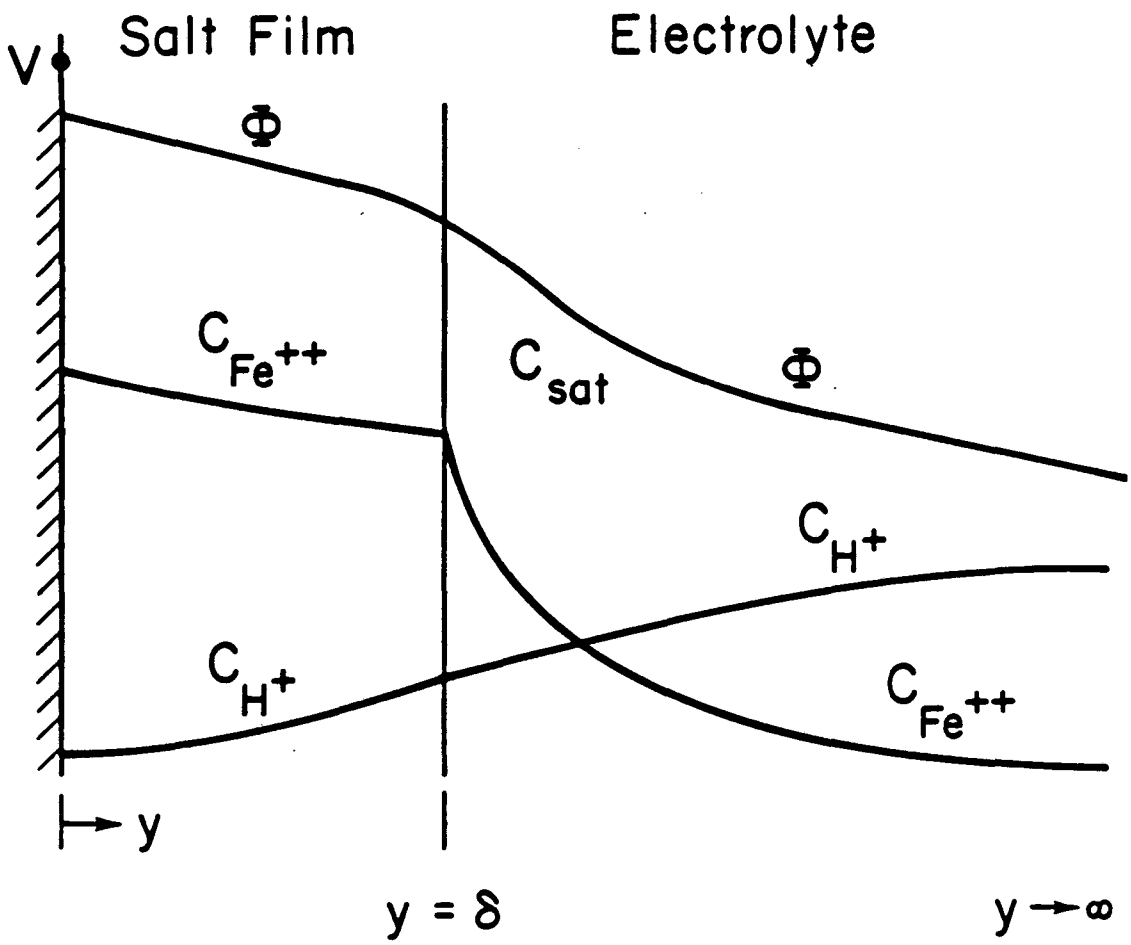

Figure 7. A steep potential gradient is present during active dissolution. Hydrogen ions migrate out of the pores of the salt film causing a transient increase in pH at the electrode-salt film interface.

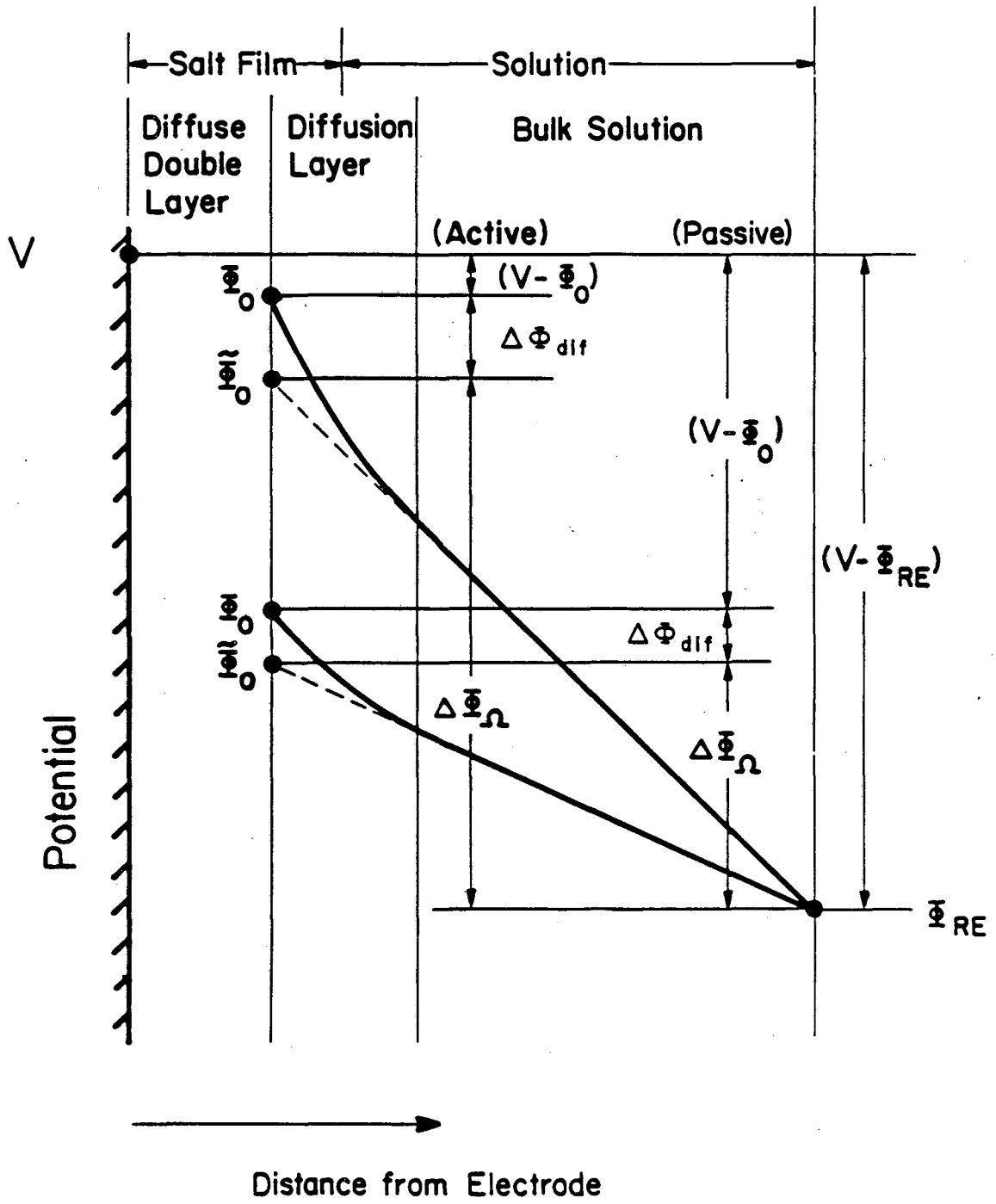

Figure 8. The quantity $V - \Phi_0$ is shown as a component of the total potential drop between the iron disk and the reference electrode. The amount of ohmic potential drop affects the value of $V - \Phi_0$.

density passive state is small; the result is a large value for $(V - \Phi_o)$.

The low passivation current generates only a small potential gradient in the salt film. This is shown in Figure 9. The hydrogen ions diffuse back into the porous salt film. The rising H^+ concentration at the oxide film-salt film interface lowers the interfacial pH. This process is characterized by line CD on Figure 6. The decrease in surface pH when the electrode is in the passive state will be referred to as phase 3. At point D, the the protective oxide film dissolves. The electrode reactivates, and the current is substantially increased. The ohmic potential drop is increased, resulting in an immediate decrease in $(V - \Phi_o)$, as seen in Figure 8. The system returns to a position near point A (Figure 6), and the cycle begins again.

The salt film always remains on the electrode surface during the oscillations. The electrode continuously cycles between phase 2 and phase 3. Phase 1, the salt-film formation process, does not enter into the oscillatory cycle.

Mathematical formulation

The governing equations presented in Part I of this series describing the salt-film-formation problem are used to model oscillations. Equations (I-41) to (I-44), (I-4), and (I-6) govern the electrolytic solution region. Equations (I-47) to (I-50), (I-4), and (I-6) govern the porous salt film region. The boundary conditions at the electrode surface and at ξ_{max} require modification.

Boundary conditions at the electrode surface

The active state current density is governed by Equation (I-28), where Equation (I-69) is substituted for $(V - \Phi_o)$, and Equation (I-64) is substituted for the superficial current density. Equation (I-63) relates the superficial current density to the pore current density and the current density determined by the Butler-Volmer equation. We previously mentioned that the

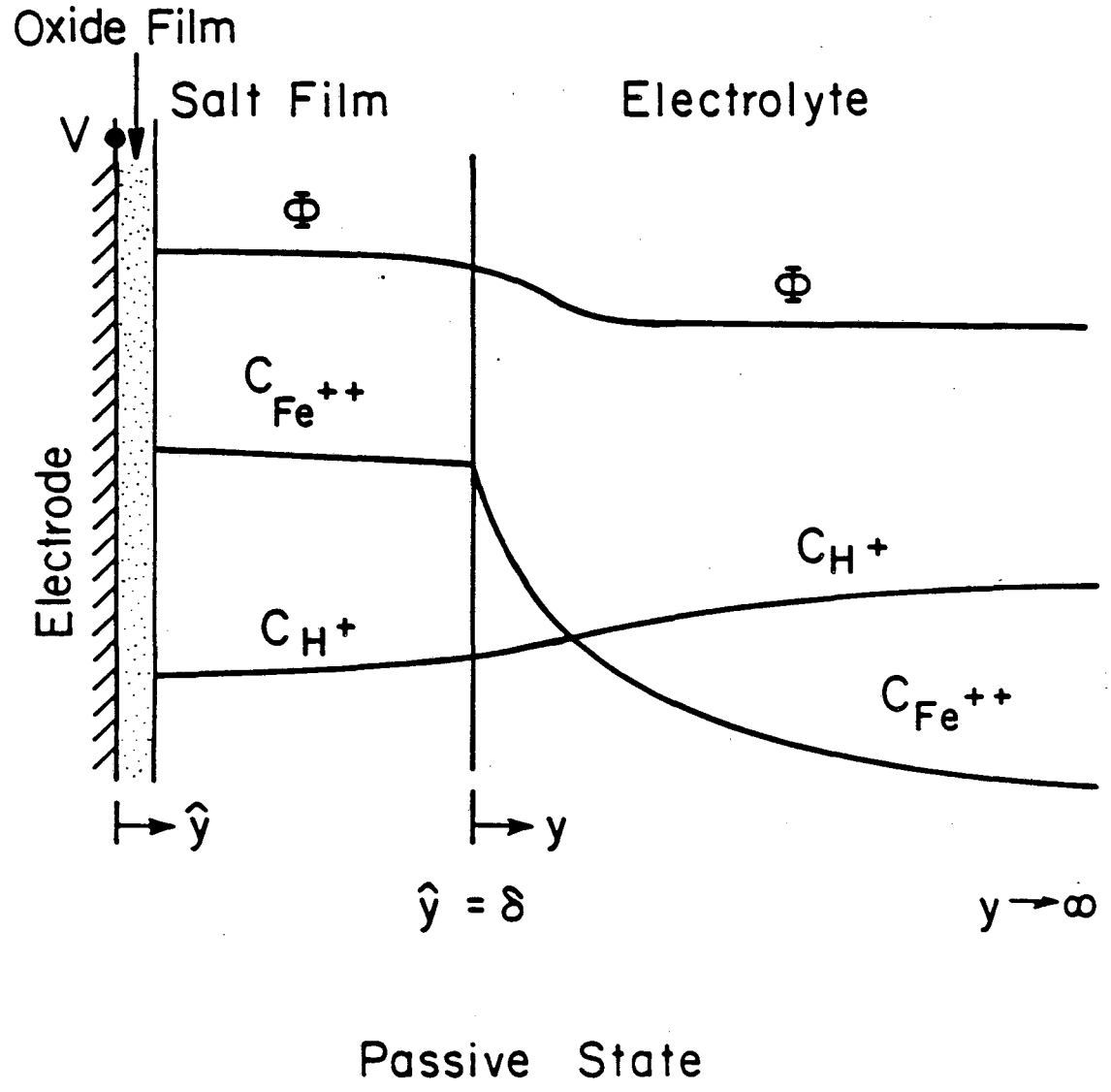

Figure 9. Hydrogen ions diffuse back into the pores of the salt film when the electrode is passivated because the electric field is substantially reduced.

concentration of ferrous ions transiently increases in the pores of the salt film, especially near the electrode surface. The maximum ferrous concentrations are found to be in the range of 6 to 8 M. These concentrations are 3 to 4 times larger than the saturation concentration of $FeSO_4$. It is likely that precipitation of $FeSO_4$ on the electrode surface will be very rapid at these concentrations. This effect is taken into account by assuming that the surface porosity is an exponentially decreasing function of the ferrous concentration, or

$$\epsilon_s = \epsilon_s^o \exp\left[-p\ (1000)\ (c_{Fe^{++}}(\eta = 0) - c^{sat}_{FeSO_4})\right]. \tag{13}$$

We will examine this assumption critically later in this paper.

The passivation current density is assumed, as a first approximation, to be a constant. The current density in the passive state is given by Equation (I-64) with $i = i_{pass} = 2\ mA/cm^2$.

Boundary conditions at ξ_{max}

The boundary conditions at ξ_{max} are selected in the same manner as described in Part I of this series for the salt-film-formation process. The dimensionless time, t, is reset to zero at the instant of initial salt-film formation. For values of $t < 1$, Equations (I-52) and (I-53) determine the outer boundary condition values. For $t \geq 1$, the bulk concentrations, represented by Equations (I-20) to (I-23), are used for the boundary conditions.

Also, for $t \geq 1$, the stretched coordinate system for the electrolytic solution, defined by Equation (I-38), is no longer required. This is because the position at ξ_{max} has moved sufficiently far from the salt film-solution interface that is is now located outside the diffusion layer in the bulk solution. It is unnecessary to continue to stretch this position because all concentrations are at their bulk values. In this case, Equation (I-38) is replaced by

$$\xi = x - \delta_x \,. \tag{14}$$

This new coordinate system is fixed relative to the salt film-solution interface. A new set of governing equations, analogous to Equations (I-41) to (I-44), is derived with this variable transformation.

In all other governing equations and boundary condition equations, t is replaced by unity when $t \geq 1$. This is the direct result of using the coordinate system given in Equation (14).

Residual ohmic drop

When the current density is at a minimum during a cycle, a certain portion of the surface remains in the active mode. This is evident because the minimum current densities on Figure 4 are larger than would be possible if the entire electrode were passive. We propose that a central region of the electrode always is in the active state. The geometry that is present at the instant of minimum current during a given cycle is illustrated in Figure 10. The small central active area is surrounded by the passive periphery.

This is in contrast to the computer model, which is one dimensional. The model applies only to regions of the electrode surface which make continuous transitions between the active and the passive states. The ohmic drop would decrease to a very small value in the computer program if the entire electrode were assumed to passivate. This is because only the passivation current density would be flowing. When the ohmic potential drop is small, $V - \Phi_o$ becomes substantially larger. In fact, $V - \Phi_o^{cp}$ would become so large under these circumstances that reactivation would require a smaller surface pH than is available in the bulk solution. This situation is impossible. The superscript cp denotes the completely passive case.

To simulate better the situation depicted in Figure 10, the program retains a residual ohmic potential drop, $\Delta\Phi_{\Omega,resid}$, when in the passive state.

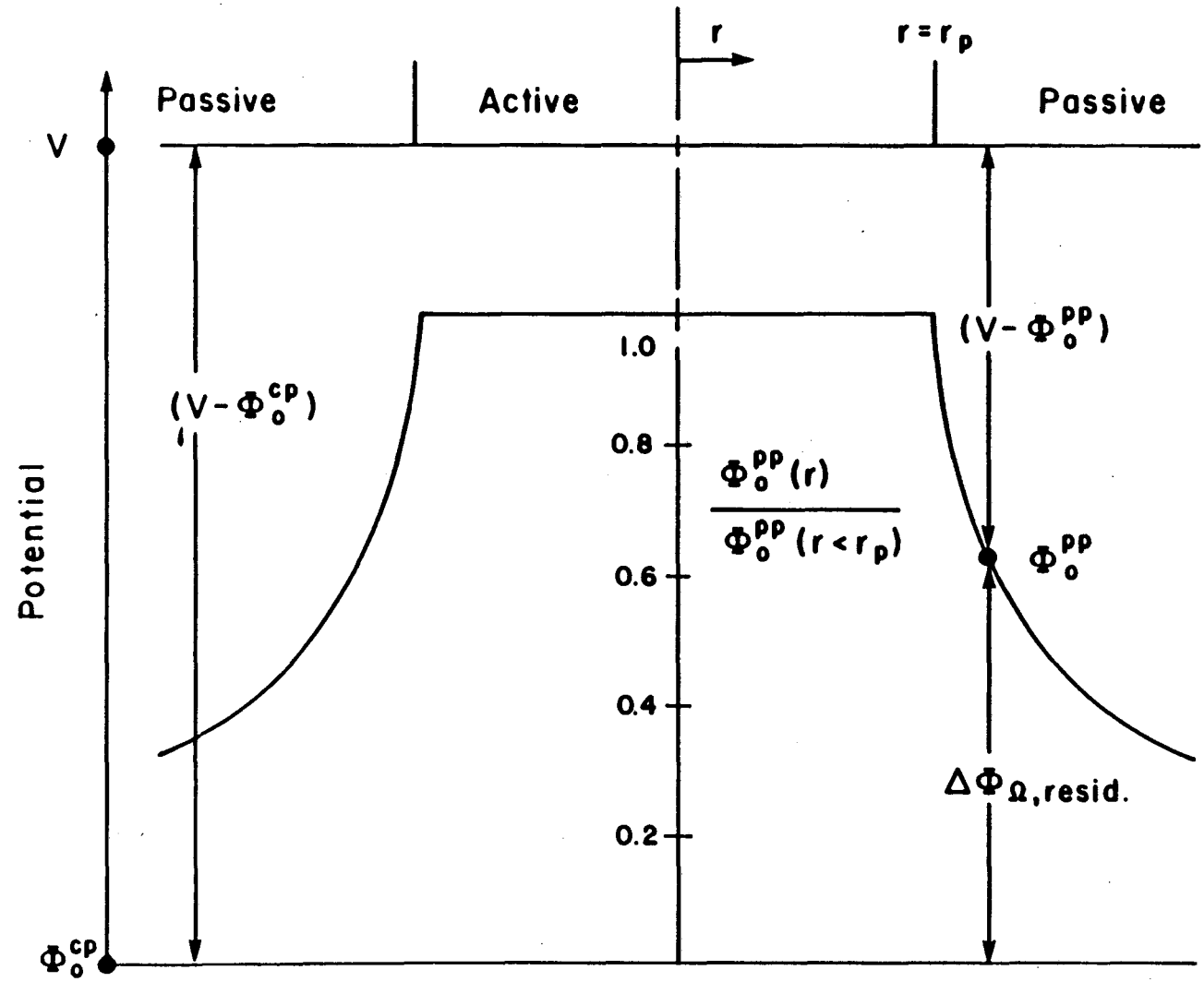

Figure 10. Residual ohmic potential drop, due to the central active portion of the electrode, prevents $(V - \Phi_o)$ for a passivated region from increasing to the value it would reach if the entire electrode was passivated.

Physically, this parameter simulates the ohmic potential drop that a partially active central region would impose on the surrounding passive region. In Figure 10, it is assumed that a primary potential distribution exists on the active part of the electrode. Φ_δ^{pp} is constant over the active portion of the electrode. The superscript, *pp*, denotes the partially passive state. As one moves radially outward over the passive region, Φ_δ^{pp} decreases.[25] A similar decrease in $\Phi_\delta^{pp}(r>r_p)$ would occur for a uniform current density on the active portion of the electrode, even though $\Phi_\delta^{pp}(r<r_p)$ would be a decreasing function of r. The residual ohmic potential drop prevents $V-\Phi_\delta^{pp}$ from increasing to the large values indicated in the previous paragraph.

Adjustment of the residual ohmic potential changes the size of the jump in $V-\Phi_o$ from point B to point C on Figure 6.

Transport property data

The transport properties and other input parameters listed in Table I of Part I of this series are used in the calculation of oscillatory behavior. Any changes from these values will be noted in the results.

Results

This section begins with a presentation of the transient changes that occur in the potential-pH conditions at the electrode surface during a cycle. All results presented are calculated with a simulated rotation speed of 167.6 rad/s and at a cell potential of $V-\Phi_{RE}$ = 0.565 V (point B on Figure 2). Current-time curves are presented for three cases which oscillated. One case in which oscillations were not observed is discussed. We discuss the qualitative similarities and the major discrepancies between the calculated results and the experimental results. It is determined that the discrepancies are due primarily to a small calculated value of the salt-film thickness. Suggestions for bringing the model results more in line with the

experimental results will then be introduced.

Table 1 lists the key input parameters and computed results for the cases to be discussed.

Cycle curves on a Pourbaix diagram

Figure 11 (a) indicates the changes in $(V - \Phi_o)$ and surface pH for cases (*i*) and (*ii*). Moving from point 1 to point 17 is a temporal progression. Point 1 is the beginning of the active dissolution process. The active dissolution results are the same for cases (*i*) and (*ii*) because they begin at the same position, point 1. The surface pH increases because hydrogen ions migrate out of the pores of the salt film in the presence of the strong electric field. The ferrous ion concentration in the pores increases; this decreases the surface porosity as described in Equation (13). The parameters used in this equation are included in Table 1. The decrease in ϵ_s requires $(V - \Phi_o)$ to

Table 1.

Values of key parameters and the computed results.

parameter or variable	dimension	case number (*i*)	(*ii*)	(*iii*)	(*iv*)
K	[mol/cm^3]	5.0x10^{-5}	5.0x10^{-5}	3.0x10^{-7}	5.0x10^{-5}
ΔV_{pass}	[V]	0.030	0.033	0.010	0.021
p	-	1.75	1.75	1.00	1.60
ϵ_s^o	-	0.01	0.01	0.02	0.01
ϵ_f	-	0.01	0.01	0.025	0.02
f	Hz	120.	44.7	192.	
δ_y	[μm]	0.735	0.657	0.766	
δ_y/ϵ_f	[μm]	73.5	65.7	30.6	

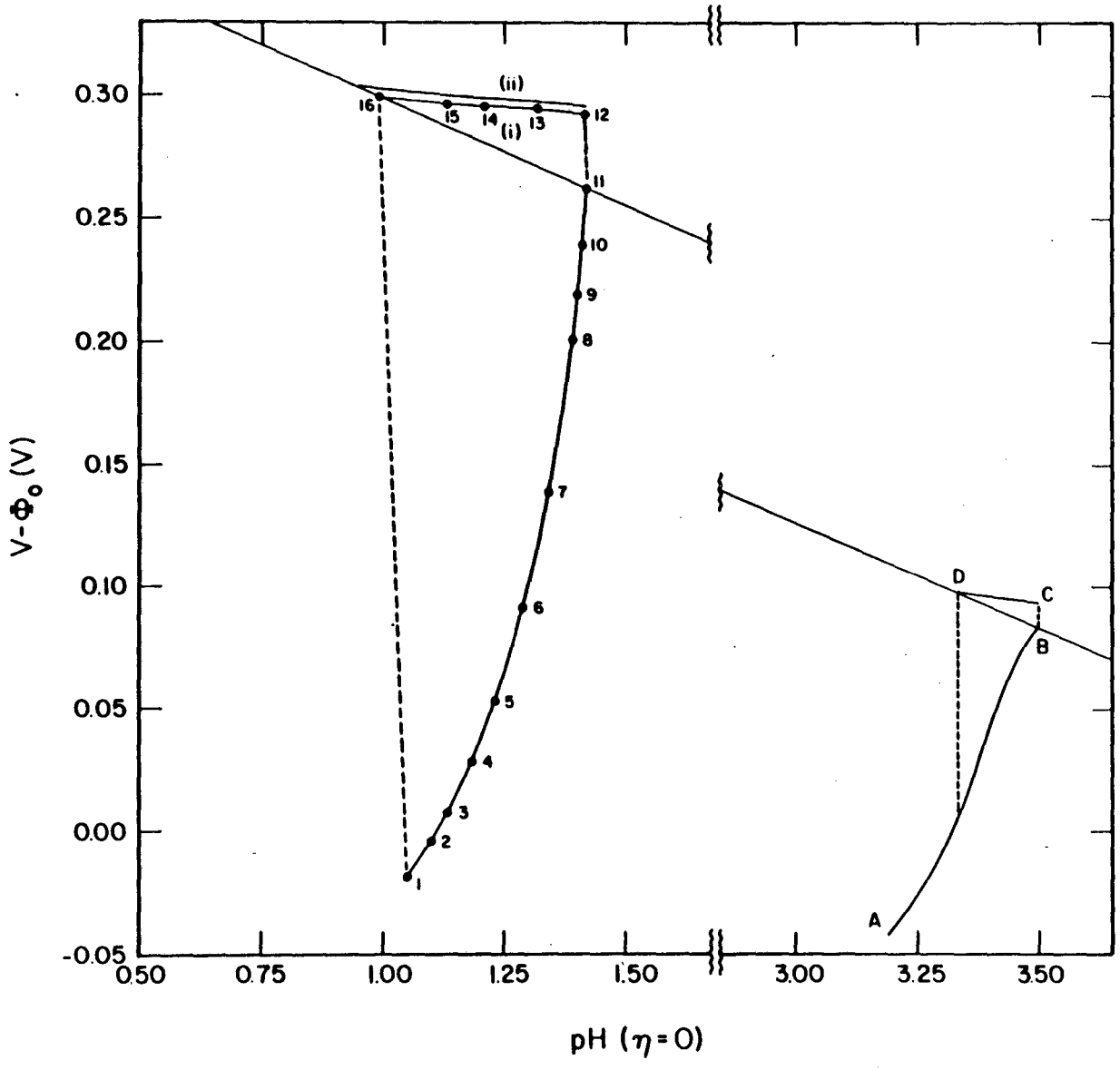

Figure 11. Calculated potential-pH conditions at the electrode surface. Part (a), cases (*i*) and (*ii*). Part (b), case (*iii*).

increase so that the specified potential difference between the working electrode and the reference electrode is maintained (potentiostatic conditions).

When point 11 is reached, the electrode passivates. The jump that occurs in $(V - \Phi_o)$ upon passivation is termed ΔV_{pass}. ΔV_{pass} is determined by the size of the residual ohmic potential drop, as discussed previously. ΔV_{pass} was equal to 0.030 V in case (*i*). ΔV_{pass} is the approximate distance between points 11 and 12 on Figure 11 (a). ΔV_{pass} was equal to 0.033 V in case (*ii*), and the increase in jump height may be observed. In both cases, the value of the pH at the electrode surface began to decrease. This is due to diffusion of H^+ ions into the salt film in the absence of a large potential gradient. The concentration profiles in the pores of the salt film begin to relax. The diffusion potential in the pores of the salt will decrease as a result of this concentration relaxation. This is responsible for the small increase in $(V - \Phi_o)$ that occurs while the electrode is in the passive state.

When point 16 is reached, the electrode will reactivate. This process is shown for case (*i*) by the dashed line from point 16 to point 17. The value of $(V - \Phi_o)$ decreases because the high active current density causes an increase in the ohmic drop. The two dashed lines on this plot indicate movements that occur instantaneously. According to the definition presented earlier in this paper, these are relaxation oscillations. Values of the dimensionless time, t, associated with each point on the cycle curve for case (*i*) are presented in Table 2.

Current-time curves

Figure 12 is the current-time curve for cases (*i*) and (*ii*) shown in Figure 11 (a). In case (i), the current density decreases during the active state. This is in agreement with the experimental current-time curves shown in Figure 4.

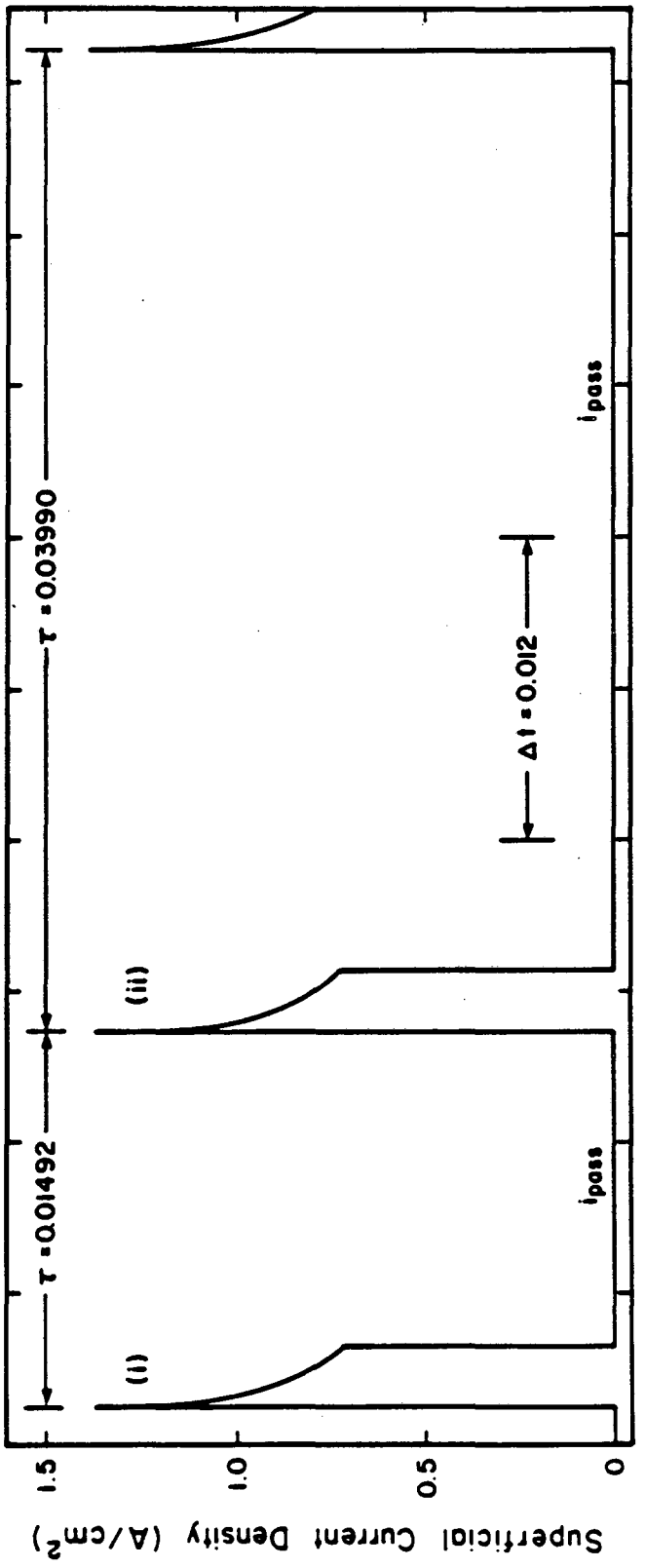

Figure 12. Calculated current-time curves for cases (*i*) and (*ii*).

Table 2.
Values of dimensionless time for various positions on cycle curve for active dissolution and passive case (*i*).

Point #	t
1	1.346×10^{-6}
2	4.505×10^{-6}
3	1.192×10^{-5}
4	2.930×10^{-5}
5	7.010×10^{-5}
6	1.658×10^{-4}
7	3.904×10^{-4}
8	9.173×10^{-4}
9	1.192×10^{-3}
10	1.550×10^{-3}
11	2.278×10^{-3}
12	2.278×10^{-3}
13	3.195×10^{-3}
14	4.432×10^{-3}
15	5.462×10^{-3}
16	1.492×10^{-2}
17	1.492×10^{-2}

The calculated current densities show good agreement with experimental values. The maximum current densities on Figure 4 are about 1.5 A/cm^2. The maximum calculated current densities are 1.38 A/cm^2. Experimentally, the current density falls to minimum values between 0.5 and 0.9 A/cm^2. The calculated current density drops off to 0.71 A/cm^2 before

passivation. The model, however, predicts $i = i_{pass}$ during passivation because of its one dimensional nature.

The experimental results indicate that the electrode remains in the active state for a longer time than it is in the passive state during a given cycle. The calculated current-time curves indicate the opposite trend. The model predicts short active times because the ferrous ion concentration builds up rapidly in the pores of the salt film. This increases the precipitation rate and decreases ϵ_s. The decrease in ϵ_s causes the potential to increase and an early passivation results.

The concentration build up process would occur more slowly for larger diffusion coefficients. The diffusion coefficients employed in this model have been reduced by a factor of four from their values at infinite dilution in order to account for the concentrated solutions that are obtained in the pores of the salt film. In the early stages of active dissolution, the ferrous ion concentration in the pores is approximately 2 M. The actual diffusion coefficients would, therefore, be larger than the values used in the program which are more appropriate for concentrations of 3 to 4 M. The calculated results would be improved if variable diffusion coefficients, which were concentration dependent, were used in the model.

Figure 12 indicates that increasing ΔV_{pass} to 0.033 V in case (ii) from 0.030 in case (i) makes the ratio of the active time to the passive time even smaller. The concentration profiles are nearly uniform in the pores of the salt film near the end of the passive part of the cycle (between points 15 and 16 on Figure 11 (a)). The driving force for interfacial pH change is low, and therefore, occurs very slowly. To make matters worse, $(V - \Phi_o)$ is increasing slightly because the diffusion potential is reduced due to the concentration profile relaxation. The size of the jump in $(V - \Phi_o)$ at passivation is limited. If it is too large, reactivation requires a surface pH value that is lower than

the pH at the salt film-solution interface. This is unlikely to occur.

The dimensionless periods of 0.01492 and 0.03990 for cases (*i*) and (*ii*) correspond to frequencies of 120 and 44.7 Hz respectively. The experimentally observed frequency is 38 Hz at this rotation speed. The close agreement in frequency between case (*ii*) and the experimental value is misleading because of the gross differences in the active time to passive time ratio for the calculated and experimental results.

Instabilities in current-time curve

Figure 4 illustrates the phenomenon of high frequency oscillations, or noise, near the positions of minimum current in the overall current-time waveform. Figure 11 shows that the potential-pH state of the electrode approaches the active passive transition boundary line very directly when the electrode is active. In the passive state the potential-pH state tends to approach the active-passive transition line in an asymptotic manner. This situation may be unstable, as the electrode may be able to jump between the active and the passive states very easily. This may explain the noise that is observed near the bottom of the current-time curves in the experimental results.

Surface porosity

Large values of $(V - \Phi_o)$ are required to passivate at low values of the interfacial pH. This fact causes some major difficulties. Point 11 on Figure 11 (a) corresponds to a value of $\epsilon_s = 6.02 \times 10^{-8}$. This value is obtained from Equation (18), with $c_{Fe^{++}} = 8.7$ M. Physically, this corresponds to nearly complete coverage of the electrode surface with $FeSO_4$ precipitate. The calculated superficial current density is 0.71 A/cm^2, as can be seen from Figure 12. This is the final active state current density occurring just before passivation. The problem is that the current density on the negligibly small

amount of free electrode surface is equal to i/ϵ_s = 1.2x10^7 A/cm^2. This value seems unrealistically large. The current density determined by the Butler-Volmer equation would be substantially reduced for a smaller value of $(V - \Phi_o)$. This can only be accomplished by having a much larger pH at the electrode surface, so that passivation may occur at a smaller value of $(V - \Phi_o)$.

A simple way of increasing the pH is to decrease the equilibrium constant in Equation (I-6). The results of this action will be described below. We will conclude that, while there is a move toward more reasonable values of the current density, the values are still about 100 times larger than the maximum current density observed by Beck[26] on newly formed metal surfaces of approximately 100 A/cm^2. This will be a starting point for a discussion of how to attack the problem in a different manner.

We decreased the equilibrium constant to 3x10^{-7} mol/cm^3. The pH values are now increased by about 2 units from the previous cases. A typical cycle curve is shown in Figure 11 (b) for this equilibrium value and the other parameters shown in Table 2 for case (*iii*). The small value of ΔV_{pass} leads to a short passivation time as shown on Figure 13. The dimensionless period corresponds to a frequency of 192 Hz, which is far greater than the 38 Hz observed experimentally. Increasing ΔV_{pass} would decrease the frequency. However, it would also decrease the active time to passivation time ratio. A decrease in the active time to passivation time ratio is contrary to the experimental results (see Figure 4).

At the instant just prior to passivation, ϵ_s was 1.2x10^{-4}, and the Butler-Volmer current density was 9.9x10^3 A/cm^2. We see that decreasing the equilibrium constant has permitted the values of ϵ_s and i_{bv} to move toward more realistic values. This indicates that further decreases in K

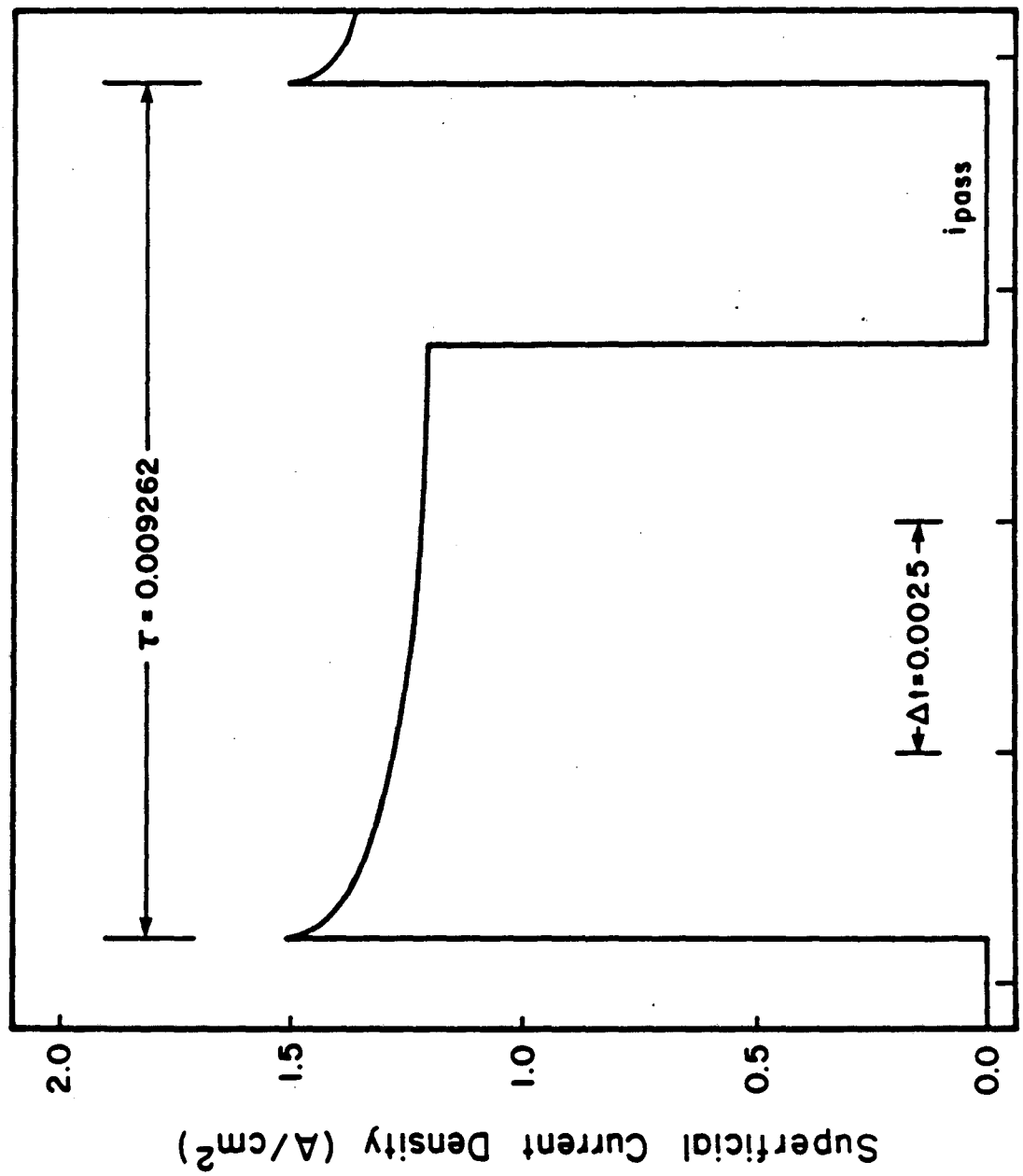

Figure 13. Calculated current-time curve for case (*iii*).

(corresponding to increases in pH) may be the way to proceed. This idea, however, must be treated with reservation. The values of K for pure H_2SO_4 solutions have previously been determined, and correlated as functions of ionic strength.[24] In case (*iii*), the value of $K = 3 \times 10^{-7}$ mol/cm^3 is more than a factor of 30 lower than the value reported at infinite dilution. This represents a lower limit on the deviation from experimental values because K has been found to be an increasing function of ionic strength[27] for pure H_2SO_4 solutions.

It seems unlikely that acidic solutions of ferrous sulfate would show the opposite behavior of pure solutions of sulfuric acid, with respect to the equilibrium constant. However, in concentrated ferrous sulfate solutions, the equilibrium constant may decrease with increasing ionic strength. If this were the case, the surface pH values would increase greatly near the electrode because of large ferrous concentrations. We would be more confident in knowing how to proceed if data were available for the bisulfate-sulfate equilibrium constant in concentrated ferrous sulfate solutions.

Salt-film dissolution kinetics

Before proceeding further, we must first ask why the calculated values of surface pH are so low. The small values of surface pH require $(V - \Phi_o)$ to reach high values in order to passivate. This is seen by noting that point 1 on Figure 11 (a) is more than 0.3 V away from the passivation potential (at the initial surface pH value of 1.05).

ϵ_s should be increased to at least 0.01 in order to keep Butler-Volmer current densities at more reasonable values. Consider the nomograph presented in Figure 3. This nomograph is constructed for the superficial current density equal to the limiting value of 1.3 A/cm^2 at Ω = 167.6 rad/s.

This would set an absolute upper limit on i_{bv} of 130 A/cm^2. For ϵ_s = 0.01 and at the limiting current, the value of $(V - \Phi_o)$ is -0.028 V. Moving to part C, at this value of $(V - \Phi_o)$, and locating the line for $V - \Phi_{RE}$ = 0.565 V indicates that δ_y/ϵ_f should have a value of 204 μm. For ϵ_f = 0.01, this corresponds to a film thickness of 2.04 μm. What are the effects of having δ_y/ϵ_f ratios different from this number? For values of $\delta_y/\epsilon_f < 204$ μm the pH change will be less than it would be for larger values of δ_y/ϵ_f. It is assumed that the decrease in H^+ concentration at the electrode surface is proportional to δ_y/ϵ_f. The numerically calculated values of δ_y/ϵ_f for the three cases we reported are listed in Table 1. This table indicates that the calculated δ_y/ϵ_f ratios are smaller than the steady-state analysis indicates they should be. This ratio may be increased by increasing the salt-film thickness or decreasing the film porosity. Beck[7] reports a porosity of 0.01 for $Fe(ClO_4)_2$ salt films. Jaenicke *et al.*[28] obtained a film porosity of 0.01 for AgCl salt films. It seems unlikely that the salt-film porosity would be able to decrease to values much lower than 0.01. At extremely low porosities, new crystal formation may rupture the film. This process may tend to keep the porosity approximately constant. If this is the case, methods for increasing salt-film thickness should be considered as the best way to bring the model results more in line with the experimental results.

The thickness of the salt film is determined by the difference between two terms:

(*i*) Material provided by dissolution of the electrode that diffuses through the porous salt film and precipitates at the film-electrolyte interface.

(*ii*) Material dissolving from the salt film into the electrolytic solution.

Presently, the model assumes that the concentration of ferrous ions at the salt film-solution interface is equal to the saturation concentration of

$FeSO_4$. This results in a more rapid rate of salt-film dissolution than if there were a limitation in this process due to the kinetics of dissolution. In this case, the dissolution rate would decrease, and the salt-film thickness would increase. This increase would be brought on by the fact that the electrode dissolution rate would now be greater than the salt-film dissolution rate. The increase in salt-film thickness would increase the surface pH due to the additional distance over which migrational forces may act on the hydrogen ions. The ohmic potential drop through the salt film will increase as the film grows thicker. This will increase the value of Φ_o. The value of $(V - \Phi_o)$ will then decrease until the rate of dissolution at the electrode matches the slower rate of dissolution of the salt film.

Beck[7] has studied salt-film growth in stagnant solutions. He has calculated a salt-film thickness of 10 μm in a 5 M $HClO_4$ solution. With ϵ_f equal to 0.01, he obtained a ratio of δ_y/ϵ_f equal to 1000 μm. This high value of δ_y/ϵ_f allows the system to have both a larger pH change through the salt film and a larger ohmic drop through the salt film. Both of these conditions will allow the system to passivate without having the large values of $(V - \Phi_o)$ which lead to unrealistically high values of the Butler-Volmer current density.

We recommend that salt-film dissolution kinetics be included in any future modeling work done on this system. Okinaka[29] has studied kinetic parameters for precipitation of cadmium hydroxide salt films. Experimental techniques similar to those described by Okinaka probably would yield kinetic dissolution parameters for the FeSO4 system. These parameters could be incorporated into a model such as the one presented here.

Case of no passivation

The last result we wish to discuss is a run obtained with the parameters listed in Table 1 under case (*iv*). The equilibrium constant returns to the value studied in cases (*i*) and (*ii*). The major difference is an increase in the film porosity to 0.02. This system never reached passivation. Passivation did not occur because the increased film porosity permits smaller pore current densities for a given superficial current density. This means that the ferrous ion surface concentration will not increase to as high a value as it would for a smaller film porosity. The surface porosity will then remain at relatively large values. Only relatively small Butler-Volmer current densities [relative to cases (*i*) and (*ii*)] were required. This caused $(V - \Phi_o)$ to be relatively small; therefore, the passivation potential was never reached.

Discussion

The purpose of this section is to analyze further the results of the previously proposed model. Specifically, the reduction in current due to the decrease in the surface porosity is compared with the reduction in current due to formation of a passive periphery surrounding an active central core as discussed in the section titled "Residual ohmic drop." The result of this comparison indicates that an oscillatory mechanism that is based on periodic changes in the surface porosity, or on periodic changes in the film porosity, should also be considered. A brief outline of these alternative models will be presented shortly.

Reduction in current

The results from cases (*i*) and (*ii*) in the "Current-time curves" section indicate that the current density decreased from 1.4 to 0.7 A/cm^2 while the electrode was in the active state. This 50% decrease is due primarily to decreases in the surface porosity. The further reduction of current due to

passivation of a peripheral region on the electrode is now approximated, and the result is compared with reduction due to lower surface porosity values.

The jump in $(V - \Phi_o)$ at passivation, ΔV_{pass}, is limited because of constraints related to reactivation conditions. These constraints were also described in the "Current-time curves" section. This limitation in ΔV_{pass} has further implications. Assume that Φ_δ^{pp} (see Figure 10) is located at r_o, the radius of the electrode. The ratio of r_o to r_p is related to ΔV_{pass} by the following equation[25]

$$\left[\left(\frac{r_o}{r_p}\right) - 1\right]^{\frac{1}{2}} = \tan\left[\frac{\pi}{2}\left(1 - \frac{\Phi_o - \Delta V_{pass}}{\Phi_o}\right)\right]. \qquad (15)$$

At point 11 on Figure 11 (a), Φ_o is equal to 0.30 V.* As an example, ΔV_{pass} is taken as 0.033 V, as it is in case (*ii*) on Table 1. Equation (15) then states that $(r_o/r_p)^2$ is equal to 1.03. This means that passivation results only in an additional 3% reduction in active area and total current.

This calculation indicates that surface blockage due to precipitated $FeSO_4$ has a greater ability to reduce the current than the presence of a passivated peripheral region on the electrode surface does.

Oscillations are observed for the hemisphere electrode. The current-time curve for the hemisphere is qualitatively similar to the current-time curves for the disks. The values of ΔV_{pass} would be even smaller for the hemisphere than for the disk. This indicates that partial passivation would be less important for the hemisphere than it would be for the disk in reducing the active area and the total current. Again, we are led to conclude that the surface blockage is responsible for reduced currents during the minimum positions on the current-time curves.

---

*This is determined by subtracting the value of $(V - \Phi_o)$ at point 11 on Figure 11 (a) from $V - \Phi_{RE}$ (= 0.565 V).

Despite this evidence, one should not completely rule out the partly active-partly passive mechanism at this time. It seems likely that a larger pH change occurs in the salt film than is presently calculated in the model. A larger pH change in the salt film would permit a larger value of ΔV_{pass} to be selected, while still permitting reactivation to occur. The larger values of ΔV_{pass} would permit the outer passivated region to be larger.

Model based on surface blockage

An alternative model that is based on periodic changes in the surface porosity will be outlined in this section. This discussion is based on the current-time curve presented in Figure 4. The location of the oscillatory region within the limiting-current plateau (Figure 2) is also considered. This model is similar to the previous model in that it assumes the presence of a porous salt film; it differs because passivation is not necessarily required in order to achieve oscillations.

Unlike the previous model, where the ferrous ion concentration was equated to the saturation concentration at the film-solution interface, the interfacial concentration is now assumed to be determined by the kinetics of dissolution or crystallization. The surface porosity is also assumed to be governed by a similar kinetic relationship.

In the high current state, the surface porosity is large. The ferrous ion concentration is rapidly increasing in the pores of the salt film near the electrode surface due to Faradaic dissolution. We now assume that the crystallization process is kinetically limited. This permits the Fe^{++} concentration near the electrode surface to greatly exceed the saturation concentration of $FeSO_4$. Once initiated, precipitation begins to block off a significant fraction of the electrode surface and decrease ϵ_s. The previous model had a 50% reduction in current density due to surface blockage, and this same phenomenon is occurring here.

The electrode is now in the low current state with most the surface covered with $FeSO_4$. As long as the pore ferrous ion concentration is greater than the saturated value, the ferrous ions have three options:

(*i*) they may precipitate on the electrode surface according to the kinetics of crystallization.

(*ii*) they may diffuse out of the pores and into the bulk solution.

(*iii*) they may diffuse out of the pores and precipitate at the film-solution interface according to the kinetics of crystallization.

The ferrous ion concentration in the pores may drop below the saturation concentration if diffusion into the bulk solution is rapid. The surface layer covering the electrode will begin to dissolve into the pore solution. If the diffusion rate out of the pores and into the bulk solution is more rapid than the kinetics of dissolution of $FeSO_4$, then the pore concentration may be reduced to a value substantially below the saturation concentration, while the electrode surface remains nearly completely covered. Continued dissolution of the surface covering layer will expose the electrode. Rapid dissolution occurs once again. However, surface blockage is delayed because of the time needed to reach a sufficient level of supersaturation in the pores to restart the kinetically impeded crystallization process. The process then repeats itself, giving rise to the oscillations.

A potential advantage of this model lies in its ability to explain the cessation of oscillations at larger cell potentials. On Figure 2, there is a region at cell potentials greater than ΔV_{osc} where oscillations cease, but the system is still at the limiting current. The present model assumes that ferrous ions may diffuse out of the pores rapidly compared to the dissolution rate of the material in the surface covering layer. The characteristic time for diffusion is on the order of $\delta_y^2 / D_{Fe^{++}}$. Figure 3, part C indicates that, for a

given value of $(V - \Phi_0)$ and a given film porosity, the salt-film thickness will increase as the cell potential is increased. The characteristic time for diffusion increases proportionally to the square of the film thickness. When the cell potential is increased from a value within ΔV_{osc} to a value greater than ΔV_{osc}, the process resulting in coverage of electrode surface is much the same. However, there are differences once the surface is covered. The rate of decrease of ferrous ion concentration in the pores is now substantially slower. If the kinetics of dissolution of the material blocking the electrode surface are now able to keep up with the diffusion process, then a steady-state condition will be reached. The flux due to Faradaic reaction occurring at the uncovered parts of the electrode surface exactly balances the diffusion flux out of the pores. The surface porosity is constant under these conditions. This results in the limiting current that is observed in Figure 2. The characteristic time for the kinetically limited dissolution is on the order of δ_y / k_d, where k_d is the kinetic rate constant with dimensions of cm/s. The value of the salt-film thickness that results in equal time constants for these two processes is D_4/k_d. For $D_4 = 0.1658 \times 10^{-5}$ cm^2/s and $k_d = 3 \times 10^{-3}$ cm/s, a critical salt-film thickness of 5.5 μm is obtained. This value of k_d was obtained by Okinaka[29] during the study of $Cd(OH)_2$ precipitation. This value of k_d is used as an order of magnitude estimate because of the lack of data for $FeSO_4$ dissolution kinetics.

Consider the events that occur as the cell potential is increased along the limiting-current plateau. The oscillatory region is followed by a steady limiting-current region, and then passivation occurs. In the surface blockage model, the system oscillates as long as the salt film is thinner than the critical value (diffusion is faster than dissolution kinetics). With increasing cell potential, the salt-film thickness increases. The oscillations then cease when diffusion becomes slower than dissolution kinetics. Further increases

in the cell potential result in additional film thickening, increases in surface pH, increases in $(V - \Phi_o)$, and finally in passivation.

In the active-passive based oscillatory model, the electrode must be subjected to conditions that permit passivation at low cell potentials in the oscillatory region. A small increase in potential to values greater than ΔV_{osc} must move the system away from conditions leading to passivation. At this time, a plausible sequence of changes in film thickness, surface pH, and potential profile that explain this phenomenon has not been developed. The surface blockage model avoids this difficulty.

The surface blockage model permits dissolution and precipitation to occur at two locations. It may occur at the salt film-solution interface, as it did in the active-passive oscillatory model. Dissolution and precipitation may also occur at the salt film-electrode interface, where is is governed by a relationship that includes kinetic inhibition.

The boundary condition equations at the salt film-solution interface and at the electrode-salt film interface that are presently in the original active-passive based oscillatory model presented here would have to be modified if this alternative model is to be tested.

Model based on variable film porosity

A more complex model describing the current oscillations is proposed in this section. Precipitation and dissolution of $FeSO_4$ are permitted at any location on the pore walls. The film porosity would now be included as a variable that depends on location in the salt film and time. Newman and Tiedemann[30] have developed equations that describe transient changes in porosity based on the fluxes at the pore wall that could be incorporated into a model of this type.

The high current state produces a high concentration of Fe^{++} ions in the pores of the salt film. This material may precipitate onto the pore walls. The pores will then decrease in size and eventually become plugged. The pore plugging process occurs gradually. The current will also decrease in a gradual manner, as observed in Figure 4. The pore concentration of Fe^{++} ions will now decrease due to diffusion into the bulk solution and the absence of the Faradaic source. The material blocking the pores will begin to dissolve. The sudden opening of the pore results in a rapid increase in current, as shown in Figure 4. At this point, the process may repeat itself.

This proposed model is similar to the variable surface porosity model in that passivation is not required to achieve oscillations. The question of coherence immediately arises. Why should most of the pores experience high rate dissolution, pore plugging, and pore opening nearly simultaneously? This question is also applicable to the variable surface porosity model, if one should decide to explore it further.

To implement the changing porosity model, significant changes would be required in the original model presented here. The film porosity will be governed by a transient material balance equation. The variable porosity must be then explicitly included in the material balance equations describing the salt-film region.

It is recommended that the experiments to determine $FeSO_4$ kinetic dissolution parameters be carried out before time is allocated to modifying the mathematical model and the associated computer program. Results from these experiments will likely indicate the most appropriate way to proceed with the modifications. We recommend that the ability of the model to predict the steady-state limiting-current behavior be carefully considered. The description of the oscillations may be approached with more confidence once the model is capable of reproducing the limiting-current behavior.

Acknowledgment

This work was partially supported by the Assistant Secretary of Conservation and Renewable Energy, Office of Energy Systems Research, Energy Storage Division of the United States Department of Energy under Contract Number DE-AC03-76SF00098. Equally important funding was received from the National Science Foundation.

List of symbols

A	electrosorbed species in the Degn model
c_i	concentration of species i, mol/cm^3
D_i	diffusion coefficient for species i, cm^2/s
F	Faraday's constant, 96,487 C/equiv
f	oscillation frequency, Hz
I	total current, A
i	superficial current density, A/cm^2
i_{bv}	current density given by Butler-Volmer eq., A/cm^2
i_p	pore current density, A/cm^2
K	bisulfate-sulfate equilibrium constant, mol/cm^3
k_d	kinetic constant for salt-film dissolution, cm/s
NHE	normal hydrogen electrode
p	parameter in surface-porosity relationship
P,Q	time independent functions in autonomous system example
R	gas constant, 8.314 J/mol-K
R	ohmic resistance, Ω
r_0	electrode radius, cm

r_p	passivation radius, cm
S	free sites for adsorption in Degn model
T	absolute temperature, K
t	dimensionless time
t^*	time, s
U^θ	standard potential, V
U^θ_{ref}	standard potential of reference electrode, V
V	electrode potential, V
$(V - \Phi_o)_*$	passivation potential, V
V_F	Flade potential, V
x	dimensionless distance from electrode
x,y	variables in autonomous system example
$\hat{x}$	$(V - V_F)$, V
y	distance from electrode, cm
z_i	charge number

Greek letters

α_a	anodic transfer coefficient
ΔV_{pass}	increase in $(V - \Phi_o)$ upon passivation, V
$\Delta\Phi_{d,f}$	diffusion potential in salt film, V
$\Delta\Phi_{d,s}$	diffusion potential in solution, V
$\Delta\Phi_{\Omega,resid}$	residual ohmic potential drop, V
ΔV_{osc}	potential range in which current oscillates, V
δ	reduced salt-film thickness
δ_x	dimensionless salt-film thickness
δ_y	salt-film thickness, cm
ϵ_f	salt-film porosity
ϵ_s	surface porosity
η	reduced distance variable in the salt film
η_c	concentration overpotential, V

κ	conductivity, $(\Omega\text{-cm})^{-1}$
κ_f	solution conductivity in salt-film pores, $(\Omega\text{-cm})^{-1}$
$\kappa_{H_2SO_4}$	conductivity of bulk solution, $(\Omega\text{-cm})^{-1}$
ξ	stretched variable in the electrolytic solution
Φ	potential in solution, V
Φ_o	potential just outside diffuse double layer, V
Φ_{RE}	potential of a reference electrode of a given kind, V
Ω	disk rotation speed, rad/s

subscripts

Hg/Hg_2SO_4	mercury-mercurous sulfate reference electrode
i	species i
o	position just outside the diffuse double layer

superscripts

cp	completely passive
pp	partially passive

References

1. P. Russell and J. Newman. "Anodic Dissolution of Iron in Acidic Sulfate Electrolytes. Part I: Formation and Growth of a Porous Salt Film." Submitted to the *Journal of the Electrochemical Society*, 1985.

2. J. Wojtowicz. "Oscillatory Behavior in Electrochemical Systems." *Modern Aspects of Electrochemistry*, **8**, Chapter 2, J. O'M. Bockris and B. Conway, eds. New York: Plenum Press, 1972.

3. D. R. Coughanowr and L. B. Koppel. *Process Systems and Control*. New York: McGraw-Hill, Inc., 1965.

4. N. Minorsky. *Nonlinear Oscillations*. Huntington, New York: R. E. Krieger Publishing Company, 1974.

5. G. Iooss and D. D. Joseph. *Elementary Stability and Bifurcation Theory*. New York: Springer-Verlag, Inc., 1980.

6. U. F. Franck and R. FitzHugh. "Periodische Elektrodenprozesse und ihre Beschreibung durch ein mathematisches Modell." *Zeitschrift für Elektrochemie*, **65** (1961), 156-168.

7. T. R. Beck. "Formation of Salt Films during the Passivation of Iron." *Journal of the Electrochemical Society*, **129** (1982), 1342-1347.

8. R. Alkire, D. Ernsberger, and T. R. Beck. "Occurrence of Salt Films during Repassivation of Newly Generated Metal Surfaces." *Journal of the Electrochemical Society*, **125** (1978), 1382-1388.

9. R. Alkire and A. Cangellari. "Formation of Salt Films during Anodic Metal Dissolution in the Presence of Fluid Flow." *Journal of the Electrochemical Society*, **130** (1983), 1252-1259.

10. H. Degn. "Theory of Electrochemical Oscillations." *Transactions of the Faraday Society*, **64** (1968), 1348-1358.

11. J. F. Cooper, R. H. Muller, and C. W. Tobias. "Periodic Phenomena during Anodic Dissolution of Copper at High Current Densities." *Journal of the Electrochemical Society*, **127** (1980), 1733-1744.

12. J. J. Podesta, R. C. V. Piatti, and A. J. Arvia. "The Potentiostatic Current Oscillations at Iron/Sulfuric Acid Solution Interfaces." *Journal of the Electrochemical Society*, **126** (1979), 1363-1367.

13. I. Epelboin, C. Gabrielli, M. Keddam, and H. Takenouti. "A Model of the Anodic Behavior of Iron in Sulfuric Acid Medium." *Electrochemica Acta*, **20** (1975), 913-916.

14. A. A. El Miligy, D. Geana, and W. J. Lorenz. "A Theoretical Treatment of the Kinetics of Iron Dissolution and Passivation." *Electrochimica Acta*, **20** (1975), 273-281.

15. J. O'M. Bockris, D. Drazic, and A. R. Despic. "The Electrode Kinetics of the Deposition and Dissolution of Iron." *Electrochimica Acta*, **4** (1961), 325-361.

16. G. Bech-Nielsen. "The Anodic Dissolution of Iron, VII: A Detailed Kinetic Model for the Two Coupled, Parallel Anodic Reactions." *Electrochemica Acta*, **21** (1976), 627-636.

17. G. Bech-Nielsen. "The Anodic Dissolution of Iron, XI: A New Method to Discern Between Parallel and Consecutive Reactions." *Electrochemica Acta*, **27** (1982), 1409-1415.

18. A. Pigeaud and H. R. Kirkpatrick. "A Correlated Potentiostatic Microscopic Study of Iron Passivation in Sulfuric Acid." *Corrosion*, **25** (1969), 209-214.

19. M. Pourbaix. *Atlas of Electrochemical Equilibria in Aqueous Solutions*. Houston, Texas: National Association of Corrosion Engineers, 1974.

20. P. Russell and J. Newman. "Experimental Determination of the Passive-Active Transition for Iron in 1 *M* Sulfuric Acid." *Journal of the Electrochemical Society*, **130** (1983), 547-553.

21. D. J. G. Ives and G. J. Janz. *Reference Electrodes*. New York: Academic Press, 1961.

22. P. Henderson. "Zur Thermodynamik der Flüssigkeitsketten." *Zeitschrift für physikalische Chemie*, **59** (1907), 118-127.

23. P. Henderson. "Zur Thermodynamik der Flüssigkeitsketten." *Zeitschrift für physikalische Chemie*, **63** (1908), 325-345.

24. J. Newman. *Electrochemical Systems*. Englewood Cliffs, New Jersey: Prentice-Hall, Inc., 1973.

25. J. Newman. "Resistance for Flow of Current to a Disk." *Journal of the Electrochemical Society*, **113** (1966), 501-502.

26. T. R. Beck. "Initial Oxide Growth Rate on Newly Generated Surfaces." *Journal of the Electrochemical Society*, **129** (1982), 2500-2501.

27. T. F. Young, L. F. Maranville, and H. M. Smith. "Raman Spectral Investigations of Ionic Equilibria in Solutions of Strong Electrolytes." *The Structure of Electrolytic Solutions*, Walter J. Hamer, ed. New York: John Wiley & Sons, Inc., 1959, pp. 35-63.

28. W. Jaenicke, R. P. Tischer, and H. Gerischer. "Die anodische Bildung von Silberchlorid-Deckschichten und Umlagerungserscheinungen nach iher Kathodischen Reduktion zu Silber." *Zeitschrift für Elektrochemie*, **59** (1955), 448-455.

29. Y. Okinaka. "On the Oxidation-Reduction Mechanism of the Cadmium Metal-Cadmium Hydroxide Electrode." *Journal of the Electrochemical Society*, **117** (1970), 289-295.

30. J. Newman and W. Tiedemann. "Porous-Electrode Theory with Battery Applications." *AIChE Journal*, **21** (1975), 25-41.

This report was done with support from the Department of Energy. Any conclusions or opinions expressed in this report represent solely those of the author(s) and not necessarily those of The Regents of the University of California, the Lawrence Berkeley Laboratory or the Department of Energy.

Reference to a company or product name does not imply approval or recommendation of the product by the University of California or the U.S. Department of Energy to the exclusion of others that may be suitable.

LAWRENCE BERKELEY LABORATORY
TECHNICAL INFORMATION DEPARTMENT
UNIVERSITY OF CALIFORNIA
BERKELEY, CALIFORNIA 94720